ORGANISATION EUROPÉENNE POUR LA RECHERCHE NUCLÉAIRE

CERN-PPE/91-19
29 January 1991

Searches for the Standard Higgs Boson produced in the reaction $e^+e^- \to H^0Z^*$.

The ALEPH Collaboration*)

Abstract

A data sample corresponding to about 185,000 hadronic Z decays collected by ALEPH at LEP has been used to search for the Standard Higgs boson produced in the reaction $e^+e^- \to H^0Z^*$. No indication for any such signal was found, and a 95% C.L. lower limit on the Higgs boson mass has been set at 48 GeV/c^2.

Contribution to the Aspen, La Thuile and Moriond conferences (Winter 1991).

*) See next pages for the list of authors.

The ALEPH Collaboration

D. Decamp, B. Deschizeaux, C. Goy, J.-P. Lees, M.-N. Minard

Laboratoire de Physique des Particules (LAPP), IN²P³-CNRS, 74019 Annecy-le-Vieux Cedex, France

R. Alemany, J.M. Crespo, M. Delfino, E. Fernandez, V. Gaitan, Ll. Garrido, P. Mato, Ll.M. Mir, A. Pacheco

Laboratorio de Fisica de Altas Energias, Universidad Autonoma de Barcelona, 08193 Bellaterra (Barcelona), Spain[9]

M.G. Catanesi, D. Creanza, M. de Palma, A. Farilla, G. Iaselli,[1] G. Maggi, M. Maggi, S. Natali, S. Nuzzo, M. Quattromini, A. Ranieri, G. Raso, F. Romano, F. Ruggieri, G. Selvaggi, L. Silvestris, P. Tempesta, G. Zito

INFN Sezione di Bari e Dipartimento di Fisica dell' Università, 70126 Bari, Italy

Y. Gao, H. Hu,[22] D. Huang, X. Huang, J. Lin, J. Lou, C. Qiao,[22] T. Ruan,[22] Wang, Y. Xie, D. Xu, R. Xu, J. Zhang, W. Zhao

Institute of High-Energy Physics, Academia Sinica, Beijing, The People's Republic of China[10]

H. Albrecht,[2] W.B. Atwood,[3] F. Bird, E. Blucher, G. Bonvicini, F. Bossi, D. Brown, T.H. Burnett,[4] H. Drevermann, F. Dydak, R.W. Forty, C. Grab, R. Hagelberg, S. Haywood, J. Hilgart, B. Jost, M. Kasemann, G. Kellner, J. Knobloch, A. Lacourt, E. Lançon, I. Lehraus, T. Lohse, D. Lüke,[2] A. Marchioro, M. Martinez, S. Menary, A. Minten, A. Miotto, R. Miquel, H.-G. Moser, J. Nash, P. Palazzi, F. Ranjard, G. Redlinger, A. Roth, J. Rothberg,[4] H. Rotscheidt, W. von Rüden, R. St.Denis, D. Schlatter, M. Takashima, M. Talby,[5] W. Tejessy, H. Wachsmuth, S. Wasserbaech, S. Wheeler, W. Wiedenmann, W. Witzeling, J. Wotschack

European Laboratory for Particle Physics (CERN), 1211 Geneva 23, Switzerland

Z. Ajaltouni, M. Bardadin-Otwinowska, A. Falvard, R. El Fellous, P. Gay, J. Harvey, P. Henrard, J. Jousset, B. Michel, J-C. Montret, D. Pallin, P. Perret, J. Proriol, F. Prulhière, G. Stimpfl

Laboratoire de Physique Corpusculaire, Université Blaise Pascal, IN²P³-CNRS, Clermont-Ferrand, 63177 Aubière, France

J.D. Hansen, J.R. Hansen, P.H. Hansen, R. Møllerud, E.R. Nielsen, B.S. Nilsson

Niels Bohr Institute, 2100 Copenhagen, Denmark[11]

I. Efthymiopoulos, E. Simopoulou, A. Vayaki

Nuclear Research Center Demokritos (NRCD), Athens, Greece

J. Badier, A. Blondel, G. Bonneaud, J. Bourotte, F. Braems, J.C. Brient, G. Fouque, A. Gamess, R. Guirlet, S. Orteu, A. Rosowsky, A. Rougé, M. Rumpf, R. Tanaka, H. Videau

Laboratoire de Physique Nucléaire et des Hautes Energies, Ecole Polytechnique, IN²P³-CNRS, 91128 Palaiseau Cedex, France

D.J. Candlin, E. Veitch

Department of Physics, University of Edinburgh, Edinburgh EH9 3JZ, United Kingdom[12]

G. Parrini

Dipartimento di Fisica, Università di Firenze, INFN Sezione di Firenze, 50125 Firenze, Italy

M. Corden, C. Georgiopoulos, M. Ikeda, J. Lannutti, D. Levinthal,[17] M. Mermikides, L. Sawyer

Supercomputer Computations Research Institute and Dept. of Physics, Florida State University, Tallahassee, FL 32306, USA[14,15,16]

A. Antonelli, R. Baldini, G. Bencivenni, G. Bologna,[6] P. Campana, G. Capon, V. Chiarella, B. D'Ettorre-Piazzoli,[7] G. Felici, P. Laurelli, G. Mannocchi,[7] F. Massimo-Brancaccio, F. Murtas, G.P. Murtas, G. Nicoletti, L. Passalacqua, M. Pepe-Altarelli, P. Picchi,[6] P. Zografou

Laboratori Nazionali dell'INFN (LNF-INFN), 00044 Frascati, Italy

B. Altoon, O. Boyle, A.W. Halley, I. ten Have, J.L. Hearns, J.G. Lynch, W.T. Morton, C. Raine, J.M. Scarr, K. Smith, A.S. Thompson, R.M. Turnbull

Department of Physics and Astronomy, University of Glasgow, Glasgow G12 8QQ, United Kingdom[12]

B. Brandl, O. Braun, R. Geiges, C. Geweniger, P. Hanke, V. Hepp, E.E. Kluge, Y. Maumary, A. Putzer, B. Rensch, A. Stahl, K. Tittel, M. Wunsch

Institut für Hochenergiephysik, Universität Heidelberg, 6900 Heidelberg, Fed. Rep. of Germany[18]

A.T. Belk, R. Beuselinck, D.M. Binnie, W. Cameron, M. Cattaneo, P.J. Dornan, S. Dugeay, A.M. Greene, J.F. Hassard, N.M. Lieske, S.J. Patton, D.G. Payne, M.J. Phillips, J.K. Sedgbeer, G. Taylor, I.R. Tomalin, A.G. Wright

Department of Physics, Imperial College, London SW7 2BZ, United Kingdom[12]

P. Girtler, D. Kuhn, G. Rudolph

Institut für Experimentalphysik, Universität Innsbruck, 6020 Innsbruck, Austria[20]

C.K. Bowdery[1] T.J. Brodbeck, A.J. Finch, F. Foster, G. Hughes, N.R. Keemer, M. Nuttall, A. Patel, B.S. Rowlingson, T. Sloan, S.W. Snow, E.P. Whelan

Department of Physics, University of Lancaster, Lancaster LA1 4YB, United Kingdom[12]

T. Barczewski, L.A.T. Bauerdick, K. Kleinknecht, B. Renk, S. Roehn, H.-G. Sander, M. Schmelling, H. Schmidt, F. Steeg

Institut für Physik, Universität Mainz, 6500 Mainz, Fed. Rep. of Germany[18]

J-P. Albanese, J-J. Aubert, C. Benchouk, V. Bernard, A. Bonissent, D. Courvoisier, F. Etienne, S. Papalexiou, P. Payre, B. Pietrzyk, Z. Qian

Centre de Physique des Particules, Faculté des Sciences de Luminy, IN²P³-CNRS, 13288 Marseille, France

H. Becker, W. Blum, P. Cattaneo, G. Cowan, B. Dehning, H. Dietl, M. Fernandez-Bosman, T. Hansl-Kozanecka,[23] A. Jahn, W. Kozanecki,[3,24] E. Lange, T. Lauber, G. Lütjens, G. Lutz, W. Männer, Y. Pan, R. Richter, J. Schröder, A.S. Schwarz, R. Settles, U. Stierlin, J. Thomas, G. Wolf

Max-Planck-Institut für Physik und Astrophysik, Werner-Heisenberg-Institut für Physik, 8000 München, Fed. Rep. of Germany[18]

V. Bertin, G. de Bouard, J. Boucrot, O. Callot[1] X. Chen, A. Cordier, M. Davier, G. Ganis, J.-F. Grivaz, Ph. Heusse, P. Janot, V. Journé, D.W. Kim,[21] J. Lefrançois, A.-M. Lutz, J.-J. Veillet, I. Videau, Z. Zhang, F. Zomer

Laboratoire de l'Accéléateur Linéaire, Université de Paris-Sud, IN²P³-CNRS, 91405 Orsay Cedex, France

S.R. Amendolia, G. Bagliesi, G. Batignani, L. Bosisio, U. Bottigli, C. Bradaschia, M. Carpinelli, M.A. Ciocci, R. Dell'Orso, I. Ferrante, F. Fidecaro, L. Foà, E. Focardi, F. Forti, A. Giassi, M.A. Giorgi, F. Ligabue, A. Lusiani, E.B. Mannelli, P.S. Marrocchesi, A. Messineo, L. Moneta, F. Palla, G. Sanguinetti, J. Steinberger, R. Tenchini, G. Tonelli, G. Triggiani, C. Vannini-Castaldi, A. Venturi, P.G. Verdini, J. Walsh

Dipartimento di Fisica dell'Università, INFN Sezione di Pisa, e Scuola Normale Superiore, 56010 Pisa, Italy

J.M. Carter, M.G. Green, P.V. March, T. Medcalf, I.S. Quazi, M.R. Saich, J.A. Strong, R.M. Thomas, L.R. West, T. Wildish

Department of Physics, Royal Holloway & Bedford New College, University of London, Surrey TW20 OEX, United Kingdom[12]

D.R. Botterill, R.W. Clifft, T.R. Edgecock, M. Edwards, S.M. Fisher, T.J. Jones, P.R. Norton, D.P. Salmon, J.C. Thompson

Particle Physics Dept., Rutherford Appleton Laboratory, Chilton, Didcot, OXON OX11 OQX, United Kingdom[12]

B. Bloch-Devaux, P. Colas, C. Klopfenstein, E. Locci, S. Loucatos, E. Monnier, P. Perez, J.A. Perlas, F. Perrier, J. Rander, J.-F. Renardy, A. Roussarie, J.-P. Schuller, J. Schwindling, B. Vallage

Département de Physique des Particules Élémentaires, CEN-Saclay, 91191 Gif-sur-Yvette Cedex, France[19]

J.G. Ashman, C.N. Booth, C. Buttar, R. Carney, S. Cartwright, F. Combley, M. Dinsdale, M. Dogru, F. Hatfield, J. Martin, D. Parker, P. Reeves, L.F. Thompson

Department of Physics, University of Sheffield, Sheffield S3 7RH, United Kingdom[12]

S. Brandt, H. Burkhardt, C. Grupen, H. Meinhard, L. Mirabito, E. Neugebauer, U. Schäfer, H. Seywerd

Fachbereich Physik, Universität Siegen, 5900 Siegen, Fed. Rep. of Germany[18]

G. Apollinari, G. Giannini, B. Gobbo, F. Liello, L. Rolandi, U. Stiegler

Dipartimento di Fisica, Università di Trieste e INFN Sezione di Trieste, 34127 Trieste, Italy

L. Bellantoni, J.F. Boudreau, D. Cinabro, J.S. Conway, D.F. Cowen,[25] A.J. DeWeerd, Z. Feng, D.P.S. Ferguson, Y.S. Gao, J. Grahl, J.L. Harton, J.E. Jacobsen, R.C. Jared,[8] R.P. Johnson, B.W. LeClaire, Y.B. Pan, J.R. Pater, Y. Saadi, V. Sharma, M.A. Walsh, J.A. Wear, F.V. Weber, M.H. Whitney, Sau Lan Wu, Z.L. Zhou, G. Zobernig

Department of Physics, University of Wisconsin, Madison, WI 53706, USA[13]

---

[1] Now at CERN.
[2] Permanent address: DESY, Hamburg, Fed. Rep. of Germany.
[3] On leave of absence from SLAC, Stanford, CA 94309, USA.
[4] On leave of absence from University of Washington, Seattle, WA 98195, USA.
[5] Also Centre de Physique des Particules, Faculté des Sciences, Marseille, France
[6] Also Istituto di Fisica Generale, Università di Torino, Torino, Italy.
[7] Also Istituto di Cosmo-Geofisica del C.N.R., Torino, Italy.
[8] Permanent address: LBL, Berkeley, CA 94720, USA.
[9] Supported by CAICYT, Spain.
[10] Supported by the National Science Foundation of China.
[11] Supported by the Danish Natural Science Research Council.
[12] Supported by the UK Science and Engineering Research Council.
[13] Supported by the US Department of Energy, contract DE-AC02-76ER00881.
[14] Supported by the US Department of Energy, contract DE-FG05-87ER40319.
[15] Supported by the NSF, contract PHY-8451274.
[16] Supported by the US Department of Energy, contract DE-FC0S-85ER250000.
[17] Supported by SLOAN fellowship, contract BR 2703.
[18] Supported by the Bundesministerium für Forschung und Technologie, Fed. Rep. of Germany.
[19] Supported by the Institut de Recherche Fondamentale du C.E.A..
[20] Supported by Fonds zur Förderung der wissenschaftlichen Forschung, Austria.
[21] Supported by the Korean Science and Engineering Foundation and Ministry of Education.
[22] Supported by the World Laboratory.
[23] On leave of absence from MIT, Cambridge, MA 02139, USA.
[24] Supported by Alexander von Humboldt Fellowship, Germany.
[25] Now at California Institute of Technology, Pasadena, California, USA.

1.- Introduction.

With the data samples collected by ALEPH at the Large Electron-Positron Collider (LEP) at CERN in 1989 and during the first half of 1990, corresponding to about 25,000 and 75,000 hadronic Z decays respectively, several analyses were performed in order to search for the standard Higgs boson over a wide mass domain.[1,2,3,4] The combination of these analyses led to the exclusion of the mass range between 0 and 41.6 GeV/c^2 at the 95% confidence level. Excluded domains up to 44 GeV/c^2 have been recently reported by the other LEP experiments.[5] The present analyses have been performed with the full data sample collected by ALEPH until September 1990 at various centre-of-mass energies during a scan of the Z peak, corresponding to about 185,000 hadronic Z decays.

Searches for many different topologies have been carried out in order to be sensitive to most of the possible final states induced by the process $e^+e^- \rightarrow H^0Z^*$. The purpose is twofold: to achieve the highest efficiency for large Higgs masses, and to increase the exclusion level of significance at lower masses (this is useful to exclude standard Higgs-like objects with weaker couplings to the Z, for example the neutral Higgs bosons of supersymmetry).

The relative Z^* decay branching ratios on the one hand (70% into hadrons, 20% into neutrinos and 10% into charged leptons) and the Higgs boson decay topologies as a function of its mass on the other have led to the following search strategy:

1.a.- Very low Higgs mass domain: $m_{H^0} < 2m_\mu$.

When the Higgs mass is less than twice the muon mass, the only available final states for its decay are e^+e^- through the direct H^0ee coupling and $\gamma\gamma$ *via* loop diagrams. Because of the weakness of the H^0ee coupling, the lifetime of such a light Higgs boson is non-negligible and has to be taken into account in the analysis; for $m_{H^0} = 40$ MeV/c^2, for instance, the lifetime is ~ 100 ps, which leads to a mean free path of ~ 6 m for a Higgs produced in the $Z \rightarrow H^0Z^*$ decay. This mean free path increases as $1/m^2_{H^0}$, making a very light Higgs practically "invisible" in Z decays. Such an invisible Higgs can be detected indirectly if the Z^* decays to an e^+e^- or $\mu^+\mu^-$ pair thanks to the missing energy-momentum in the event.

The search for the relevant topology, an energetic acoplanar lepton pair†, is reported in Section 3.

1.b.- Intermediate Higgs mass domain: $2m_\mu < m_{H^0} < 15\ GeV/c^2$.

For m_{H^0} smaller than twice the D mass, the main Higgs decay topology is into two charged particles. Therefore, a search for acoplanar charged particle pairs with substantial missing energy is relevant when $Z^* \rightarrow \nu\bar{\nu}$. This topology is also characteristic

† If the *tau*-neutrino were massive, the Higgs boson would also decay into a ν_τ pair and this search would apply equally well.

of the configuration $(H^0 \rightarrow \tau^+\tau^-)(Z^* \rightarrow \nu\bar{\nu})$. Such a search, extended to be made sensitive to the 3-prong decay of the *tau*, is described in Section 4.

In the configuration $(H^0 \rightarrow \tau^+\tau^-)(Z^* \rightarrow l^+l^-)$, where l is a lepton, a search for 4-lepton final states is relevant and is presented in Section 5.

For higher Higgs masses, the charged multiplicity of the decay products increases and the dominant final state becomes a hadronic jet. In the configuration $(H^0 \rightarrow hadrons)(Z^* \rightarrow \nu\bar{\nu})$ and in the Higgs mass range considered, the typical Higgs momentum is sufficiently large with respect to m_{H^0} for the monojet topology to be dominant: it still accounts for 80% of the final states when $m_{H^0} = 15$ GeV/c^2. The search for such a topology is reported in Section 6.

1.c.- High Higgs mass domain: $m_{H^0} > 11$ *GeV*/c^2.

Above the $b\bar{b}$ threshold, the dominant Higgs decay mode is into hadrons, but the branching ratio into *tau* pairs always remains above 6%. Therefore, the searches for acoplanar *tau* pairs and for 4-lepton final states remain relevant.

Although the search for monojets retains substantial efficiency up to about 35 GeV/c^2, a search for pairs of acoplanar, acollinear jets with missing energy becomes increasingly appropriate in the configuration $(H^0 \rightarrow hadrons)(Z^* \rightarrow \nu\bar{\nu})$ as the Higgs mass gets larger. This search is described in Section 7.

When the Z^* decays into two electrons or two muons instead of neutrinos, the topology to be searched for is a pair of energetic, isolated (and thus well identifiable) leptons in hadronic events. This search is presented in Section 8.

When the Z^* decays into two *taus*, a fraction of the energy of the *taus* is carried away by the decay neutrinos. Depending on this fraction, the possible final state topologies are very different. In one extreme situation, the final state resembles the configuration $(H^0 \rightarrow hadrons)(Z^* \rightarrow \nu\bar{\nu})$, and the search for acoplanar jets therefore applies. In another extreme situation, the two *taus* may decay into energetic electrons or muons and the search for energetic leptons can be used. When the two *taus* decay into energetic charged particles, but now not necessarily leptons, the final state may be characterized by two charged particles isolated from a hadronic system. The corresponding search is reported in Section 9. Finally, when the energy of one of the *taus* is carried mainly by a charged particle, while the energy of the other mainly by neutrinos, a search for isolated charged particles in hadronic events is performed, as described in Section 10. Of course, all these searches apply equally well in the configuration $(H^0 \rightarrow \tau^+\tau^-)(Z^* \rightarrow hadrons)$.

In Section 11, the efficiencies and the numbers of events expected to be selected by each of these searches, as a function of m_{H^0}, are summarized, and a new lower limit on the Higgs mass is inferred.

2.- Common features and definitions.

A detailed description of ALEPH can be found in Ref. 6, and a brief account, together with the relevant trigger conditions, in Ref. 3 for instance.

2.a.- Charged particles tracks.

To be used in the present analyses, charged particle tracks are required to be reconstructed with at least four space coordinates in the TPC, and to originate from the beam-crossing point within 7 cm along the beam direction and 2.5 cm in the transverse direction. Furthermore, to be counted as "good tracks", they must form with the beam direction an angle of at least 18.2°.

For charged particle tracks not originating from the main interaction point, a secondary vertex (V^0) reconstruction is attempted. The tracks belonging to a reconstructed V^0 pointing to the interaction vertex within the same tolerances as those defined for good tracks are taken into account, for instance in the determination of the total energy, but they are not counted as good tracks.

2.b.- Calorimetric clusters.

In both electromagnetic (ECAL) and hadronic (HCAL) calorimeters, clusters are defined as groups of hit cells topologically connected. The energy of a cluster is the sum of the energies measured in its cells. To be validated, an ECAL cluster is required to have an energy compatible with the energy independently measured on the wire planes in the corresponding ECAL module, and a HCAL cluster has to be topologically connected to a pattern of hit streamer tubes in the corresponding HCAL module. The validated ECAL clusters can be identified as electromagnetic or hadronic clusters thanks to the granularity of the calorimeter (the typical cell size is smaller than $1° \times 1°$), and taking advantage of the characteristic longitudinal and transverse profiles of electromagnetic showers. To be considered in the subsequent analyses, the photon-like clusters are required to carry more than 200 MeV and the neutral hadron-like ones to carry more than 500 MeV.

2.c.- Energy flow algorithm.

For the final states with missing energy (involving neutrinos from Z^* or from *tau* decays), an energy flow algorithm has been developed, making use of the information coming from most of the ALEPH subdetectors. In particular, advantage is taken of the photon, electron and muon identification capabilities and of the redundancy of the energy measurements in the calorimeters. The principles of the energy flow algorithm are described in Ref. 4. A relative energy resolution of $\sim 9\%$ is achieved, practically independent of the energy.

2.d.- Particles.

All the good tracks, tracks from reconstructed V^0s, photons and neutral hadrons provided by the energy flow algorithm are called "particles" in the following. These particles are used in the analyses to determine quantities like missing momentum, visible mass, thrust axis, etc.

2.e.- Jets.

The events are divided into two hemispheres by a plane perpendicular to the thrust axis, two jets being thereby defined. The acollinearity η is the angle between the two jet directions, and the acoplanarity ψ the angle between the two jet directions projected onto $\mathcal{P}$, the plane transverse to the beam axis.

In the case of events induced by two-photon processes or by annihilation accompanied by hard initial state radiation, it may be preferable to work directly in the plane $\mathcal{P}$. For that purpose, all particle momenta are projected onto $\mathcal{P}$, a 2d-thrust axis is computed therein, and the event is divided into two 2d-jets with respect to that axis. The projected acoplanarity ψ_p is defined as the angle between the directions of the two 2d-jets. The projected transverse momentum ρ_p is defined as the scalar sum of the transverse components of the 2d-jet momenta, measured with respect to the 2d-thrust axis.

A given part of an event may also be "forced to n jets", the clusterization being in that case performed with the LUCLUS algorithm.[7]

2.f.- Energy in the forward direction E_{12}.

Although it is instrumented down to a polar angle of 2°, the very forward region of the detector, including ECAL/HCAL edges and the luminosity calorimeter (LCAL), is preferably avoided in the missing energy channel analyses since the boundaries between calorimeters are more numerous in this region and the energy resolution is therefore degraded. For vetoing purposes, the quantity E_{12}, defined as the total energy measured in the calorimeter cells (summed over validated clusters) within 12° of the beam axis, is used.

2.g.- Veto inefficiencies.

When the calorimeters are used to veto events (see E_{12} in Section 2.f for instance), the possibility of vetoing a signal event because of a spurious energy deposit in any of the calorimeters has to be accounted for. The related inefficiencies have been systematically determined using events triggered at random beam crossings.

2.h.- Normalization.

The numbers of multihadronic decays recorded at each energies have been obtained by counting the events with at least five good tracks and carrying a scalar sum of momenta in excess of 10% of the centre-of-mass energy, when all the components of the detector were simultaneously in good working condition. The efficiency of this selection has been determined to be $97.5 \pm 0.6\%$,[8] with a background coming from $e^+e^- \to \tau^+\tau^-$ of 0.3% and from $e^+e^- \to (e^+e^-)$ *hadrons* of less than 0.05% at the peak energy. These numbers of events, before and after background subtraction and efficiency correction, are listed in Table 1. Also shown in this Table are the integrated luminosities obtained by dividing the numbers of hadronic decays by the hadronic cross section predicted by the Standard Model. These integrated luminosities have been used in the computation of the expected number of events from the $e^+e^- \to H^0Z^*$ process, thus making the prediction largely independent of theoretical uncertainties common to the $e^+e^- \to q\bar{q}$ and the $e^+e^- \to H^0Z^*$ cross sections (the latter has been determined as described in Ref. 1).

Table 1. Numbers of hadronic events and luminosities recorded at each centre-of-mass energy.

$\sqrt{s}$ (GeV)	N_{had}	N^*_{had}	$\mathcal{L}$ (pb^{-1})
88.227	4,383	4,443	0.972
89.230	6,001	6,109	0.710
90.233	12,750	13,013	0.702
91.032	4,795	4,898	0.165
91.222	120,105	122,687	4.012
91.532	4,619	4,717	0.159
92.226	15,476	15,799	0.734
92.562	60	60	0.003
93.225	8,882	9,055	0.726
94.223	7,873	8,012	0.996
95.040	208	211	0.038
Total	185,152	189,004	9.217

N_{had} is the number of events satisfying the hadronic selection criteria (see text).
N^*_{had} is the corrected number of hadronic events (see text).

2.i.- Monte Carlo samples.

In order to avoid biasing the determination of the confidence levels and of the corresponding Higgs mass limit, the selection procedures have been developed using appropriately weighted samples of fully simulated events, so that the efficiency for

the H^0Z^* search is maximized while less than 1 background event is expected to be observed in the data sample. The Monte Carlo samples used are:

- 265,000 $Z \rightarrow hadrons$,
- 30,000 $Z \rightarrow \tau^+\tau^-$, corresponding to three times the recorded integrated luminosity,
- 30,000 $e^+e^- \rightarrow (e^+e^-)q\bar{q}$, with $m_{q\bar{q}} > 4$ GeV/c^2, corresponding to an integrated luminosity of $\sim 25\text{pb}^{-1}$,
- 20,000 $e^+e^- \rightarrow (e^+e^-)\tau^+\tau^-$, corresponding to an integrated luminosity of ~ 50 pb^{-1},
- and, for various Higgs masses from 0 to 60 GeV/c^2, at least 1,000 H^0Z^* events in each of the configurations studied. In these simulations, initial and final state radiations are included, and the various Higgs decays are computed and simulated as described in Ref. 1.

The same selection procedures have subsequently been applied to the data. A complete example of such a background study is given in Section 7 where the acoplanar jet selection is described.

3.- Search for energetic acoplanar pairs.

In this section, a search for energetic lepton pairs with missing energy, typical of a long-lived Higgs boson, is described. The backgrounds to such final states are $Z \rightarrow \tau^+\tau^-$, with each of the *taus* decaying to a single charged particle, $Z \rightarrow l^+l^-(\gamma)$, with $l = e$ or μ, and charged particle pairs produced in two-photons interactions.

In the data sample, $\sim 67,000$ events have exactly two good tracks and are considered. The $Z \rightarrow \tau^+\tau^-$ background is brought down to a negligible level by requesting that both charged particle momenta exceed 30 GeV/c. This same cut also removes the numerous but low energy lepton pairs produced in two-photons interactions. This led to $\sim 27,000$ events in the data.

Non-radiative dilepton events and dilepton events where a photon from initial or final state radiation is present but remains undetected because it is emitted below the LCAL acceptance or too close to the direction of one of the final leptons (in which case its energy deposit in ECAL is not resolved from that of the charged lepton), are eliminated by cuts on the acoplanarity and on the acollinearity angles of the two leptons respectively: both $\pi - \eta$ and $\pi - \psi$ are requested to exceed 50 mr. Only 364 events remained at this stage.

The other radiative dilepton events are eliminated by requesting that E_{12} be zero, that the total energy of the validated ECAL neutral clusters be less than 1 GeV, and that the total energy of the validated HCAL neutral clusters situated in the regions of HCAL backing the boundaries between the ECAL modules be less than 500 MeV. In order to avoid vetoing a Higgs event because of a final state radiation or Bremsstrahlung photon coming from one of the two leptons, the calorimetric clusters situated within $\pm 2°$ in polar angle and within $+Q_l \times 6°$ and $-Q_l \times 3°$ in azimuth of the direction of the charged particles are ignored (Q_l is the sign of the charge of the particle). Asymmetric azimuthal cuts are used because of the curvature of the charged particle tracks in the magnetic field.

No events survived in the data, while the efficiency of this selection for a massless, and therefore stable, Higgs boson is 30% when Z^* decays to $\mu^+\mu^-$ and 20% when Z^* decays to e^+e^-, including a 2.5% inefficiency related to the calorimetric vetos. When the Higgs mass is non-zero, an additional factor in the efficiency has to be introduced to take into account the finite Higgs lifetime.

4.- Search for acoplanar pairs.

In this section, the topology of interest consists of a pair of charged particles or *tau* decay products accompanied by missing energy. The search has been optimized for a 50 GeV/c^2 Higgs boson in the configuration $(H^0 \rightarrow \tau^+\tau^-)(Z^* \rightarrow \nu\bar{\nu})$, but it is also used for the two- or four-prong Higgs boson decays that occur below the $\tau^+\tau^-$ threshold.

To select this topology, events with 2 or 4 charged particle tracks and total electric charge zero are considered. *Tau* candidates decaying into three charged particles are selected as triplets of tracks with a total electric charge ± 1 and an invariant mass smaller than 1.5 GeV/c^2 (the pion mass being assumed for the charged particles). If more than one triplet fulfil these conditions, only the one with the lowest mass is considered. For simplicity, the *tau* triplets and the remaining charged particle tracks are referred to as *leptons*, and only the events with two *leptons* are further considered. In the data, about 70,000 events satisfy the above preselection criteria. At this stage, the main background sources are $e^+e^- \rightarrow l^+l^-(\gamma)$ and $e^+e^- \rightarrow (e^+e^-)l^+l^-$.

To avoid energy losses in the forward region of the detector, E_{12} is required to be zero and both *lepton* directions must form an angle θ with the beam axis such that $|\cos\theta| < 0.95$.

The acollinearity angle of the two *leptons*, η, must be smaller than 165°. This removes most of the $Z \rightarrow l^+l^-$ events. In addition, if the angle θ between the direction of the total momentum of the *leptons* and the beam axis is such that $|\cos\theta| < 0.90$, it is required that $\eta > 2.5°$; this is to remove e^+e^- pairs from photon conversions which occur preferentially at low angles with respect to the beam axis.

Events from $Z \rightarrow l^+l^-\gamma$ are eliminated by applying a "photon veto" which requires that no neutral particle with energy above 1 GeV be detected unless the angle of its direction with that of one of the *leptons* is smaller than 10°, or unless the invariant mass between it and one of the *leptons*, assumed to be massless in this computation, is smaller than 2 GeV/c^2. These protections avoid vetoing an event because of a photon coming from a τ decay. In addition, in order to keep low multiplicity monojets, the "photon veto" is not applied to events with a total visible mass smaller than 10 GeV/c^2. About 18,000 events remained at this stage.

The component of the vector sum of the *lepton* momenta transverse to the beam axis must exceed 3.75% of the centre-of-mass energy. The same cut is applied to the transverse component of the total visible momentum. These cuts remove most of the background from two-photon events in which both spectator electrons remain below the inner boundary of the LCAL acceptance. As it may also happen that a spectator electron escapes through the vertical crack of the LCAL, but still remains below the inner boundary of the HCAL

acceptance, a tighter cut at 5% of the centre-of-mass energy is applied, but only if the direction of the total missing momentum is within $\pm 10°$ in azimuth of the vertical LCAL crack. This led to 61 events observed in the data.

The background from $e^+e^- \to (e^+e^-)\tau^+\tau^-$ is not fully removed by the transverse momentum cuts because of the energy taken away by the neutrinos from the τ decays. These events appear almost coplanar, but with an acoplanarity potentially increased if at least one of the *taus* has emitted an energetic neutrino. This background is efficiently removed by requiring that the projected transverse momentum ρ_p be smaller than 1.25 GeV/c (see Fig. 4.1). To preserve monojet-like events, this last cut is not applied when the 2d-thrust axis points between the two projected *lepton* momenta.

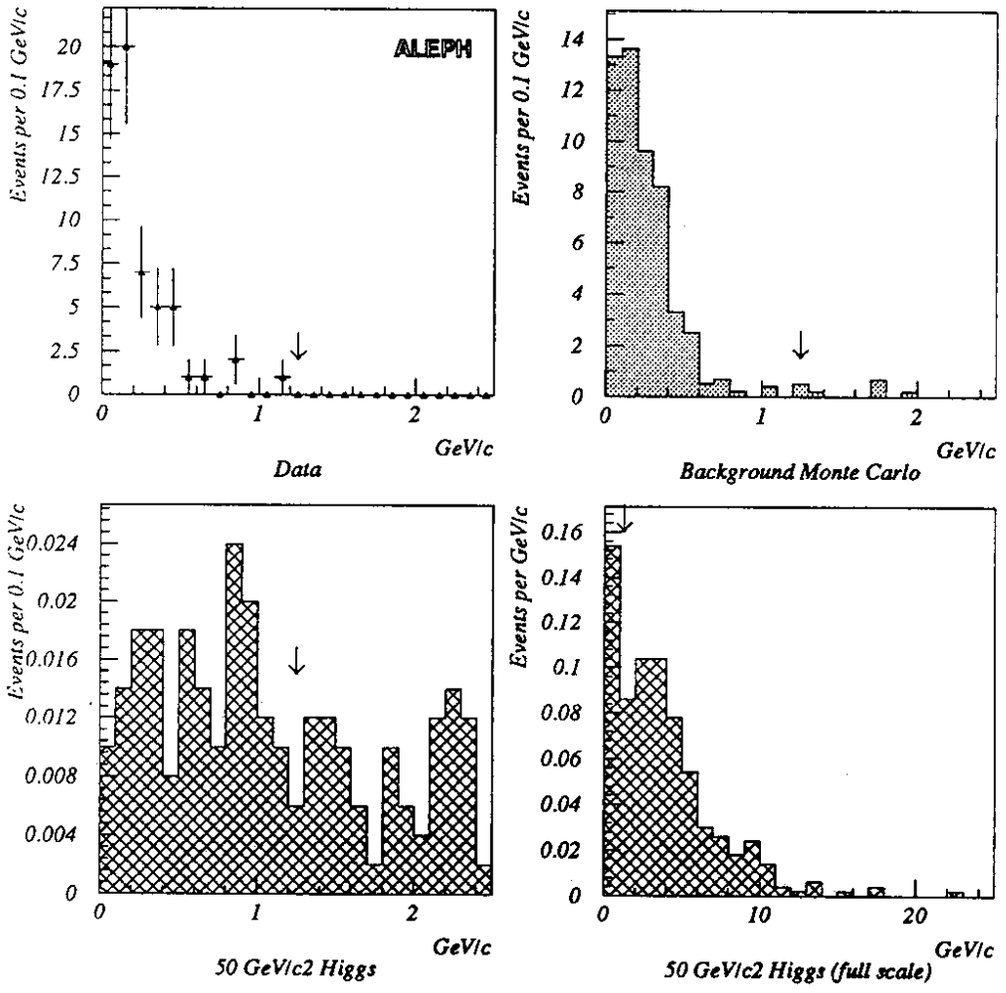

Fig.4.1 Projected transverse momentum distibutions

No events remained, while the efficiency for a 50 GeV/c^2 Higgs boson decaying to $\tau^+\tau^-$, with the Z^* decaying to $\nu\bar{\nu}$, is 41% including a 2.5% veto inefficiency determined as described in Section 2.g.

5.- **Search for four-lepton final states.**

To select this topology, only events with 4 or 6 charged particle tracks are considered, and among them, only those with four *leptons*, as defined in Section 4, are kept. The same E_{12} veto is also applied.

For the 1034 events passing this preselection, it was requested that all *lepton* pair invariant masses exceed 2 GeV/c^2 (in this computation, the *leptons* are considered massless). Only 4 events fulfil these criteria, all identified as $ee\mu\mu$ and $\mu\mu\mu\mu$ final states. These events were removed by further requesting that the scalar sum of the charged particle momenta be less than 85 GeV/c. In Higgs events, it is expected that a substantial energy, carried away by the neutrinos from τ decays, should be missing. For a 50 GeV/c^2 Higgs boson decaying to $\tau^+\tau^-$ while the Z^* decays to e^+e^-, $\mu^+\mu^-$ or $\tau^+\tau^-$, the efficiency of this search is 54% (including a 2% veto inefficiency).

6.- **Search for monojets.**

The main backgrounds to the monojet topology are two-photon processes and $e^+e^- \rightarrow \tau^+\tau^-$ when the energy of one of the *taus* is carried away by neutrinos. To reject most of the latter, only events with at least 4 good tracks are considered. For an event to be classified as a monojet, one of the two hemispheres defined with respect to the thrust axis is required to contain an energy smaller than 2 GeV, the other hemisphere being the "monojet". At this preselection level, 4032 events were observed.

By reinforcing the veto on the second hemisphere in requiring that no energy be measured in a cone of half angle 50° around the direction opposite to that of the monojet, most of the $e^+e^- \rightarrow$ *hadrons* and all of the remaining $e^+e^- \rightarrow \tau^+\tau^-$ background events are removed.

This leads to 2568 events which come mostly from two-photon processes and are expected to be produced at low polar angle. Therefore, the direction of the monojet is required to form an angle θ with respect to the beam axis such that $|\cos\theta| < 0.9$ and E_{12} must be zero, rejecting that way more than 95% of the background and leading to 60 events observed.

No events survived in the data after requesting that the total transverse momentum exceed 5% of the centre-of-mass energy. This cut eliminates most of the remaining background, as shown in Fig. 6.1 (the apparent disagreement between data and expectation in the overall normalization can be attributed to the $m_{q\bar{q}} > 4$ GeV/c^2 cut-off in the simulation of the two-photon processes). Finally, to remove the few background events still expected from the process $e^+e^- \rightarrow (e^+e^-)\tau^+\tau^-$, and although this is not needed by the data, the projected acoplanarity ψ_p is required to be smaller than 150°.

For a 11 GeV/c^2 Higgs, the resulting efficiencies are 57% when $H^0 \rightarrow$ *hadrons* and 13% when $H^0 \rightarrow \tau^+\tau^-$ (which occurs at this mass in 25% of the cases). These efficiencies include a 2.5% veto inefficiency determined as described in Section 2.g.

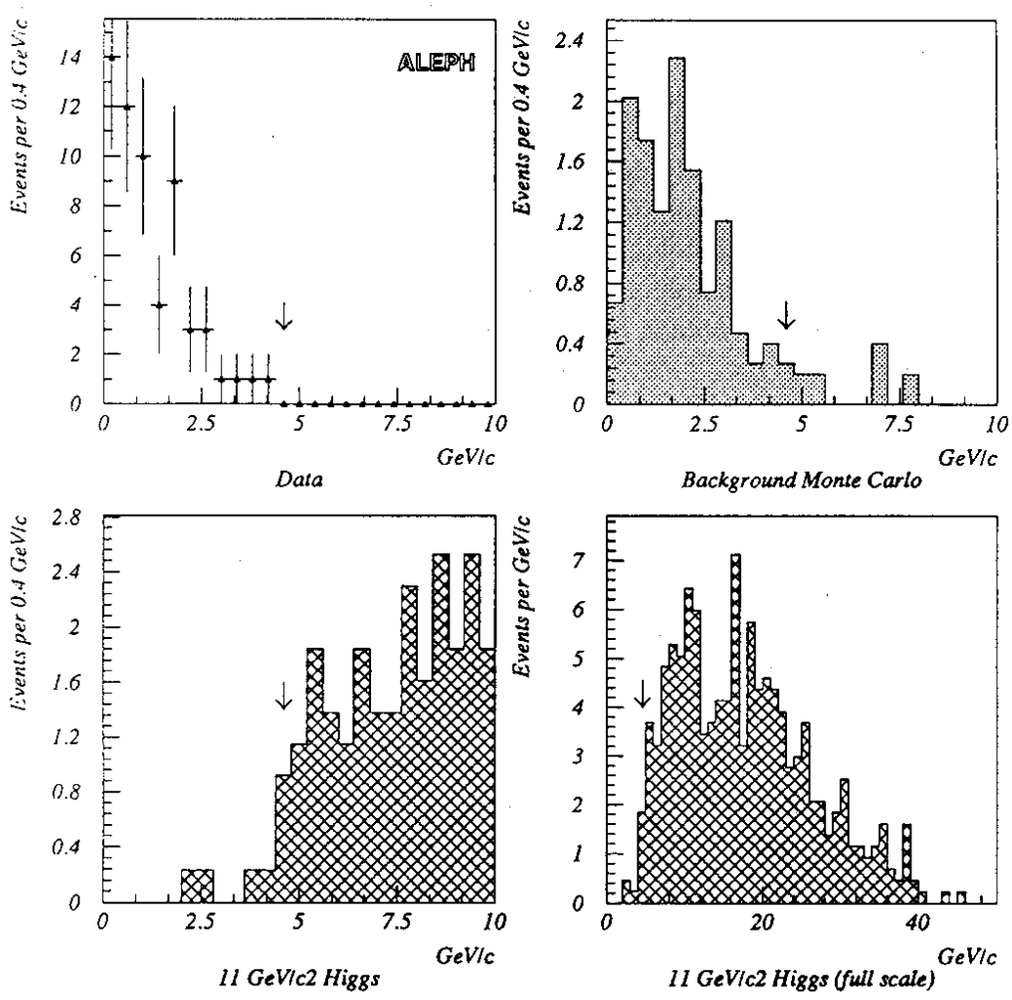

Fig.6.1 Total transverse momentum distributions.

7.- Search for acoplanar jets.

In this section, the topology of interest consists of a pair of jets accompanied by missing energy. The search has been optimized for a 50 GeV/c^2 Higgs boson in the configuration $(H^0 \rightarrow hadrons)(Z^* \rightarrow \nu\bar{\nu})$.

Backgrounds to this process arise from events where some energy is either unseen or mismeasured by the detector. Therefore, performing cuts on energy related quantities might not be the best choice to get rid of standard sources of missing energy. However, as this missing energy is likely to be contained in jets (neutrinos from semileptonic decays, cracks in the calorimeters), the directions of the jets should still be well determined and reliable. Most of the cuts were thus performed on these directions, resulting in both a higher selection efficiency and a better selectivity.

To design these cuts, attention was first focused on hadronic events with energy actually lost, characterized by a visible mass smaller than 70 GeV/c^2, at least 5 good tracks and a scalar sum of the momenta carried by the good tracks in excess of 8 GeV/c. In addition, to be complementary to the monojet analysis (see Section 6), the energies measured in the two hemispheres defined with respect to the event thrust axis are required to exceed 2 GeV. At this level, 11,390 events are expected from $e^+e^- \to q\bar{q}$, 200 from $e^+e^- \to \tau^+\tau^-$ and 255 from $e^+e^- \to (e^+e^-)$*hadrons*, while 11,865 were seen in the data. Expected and observed visible mass distributions are also in good agreement, as shown in Fig. 7.1.

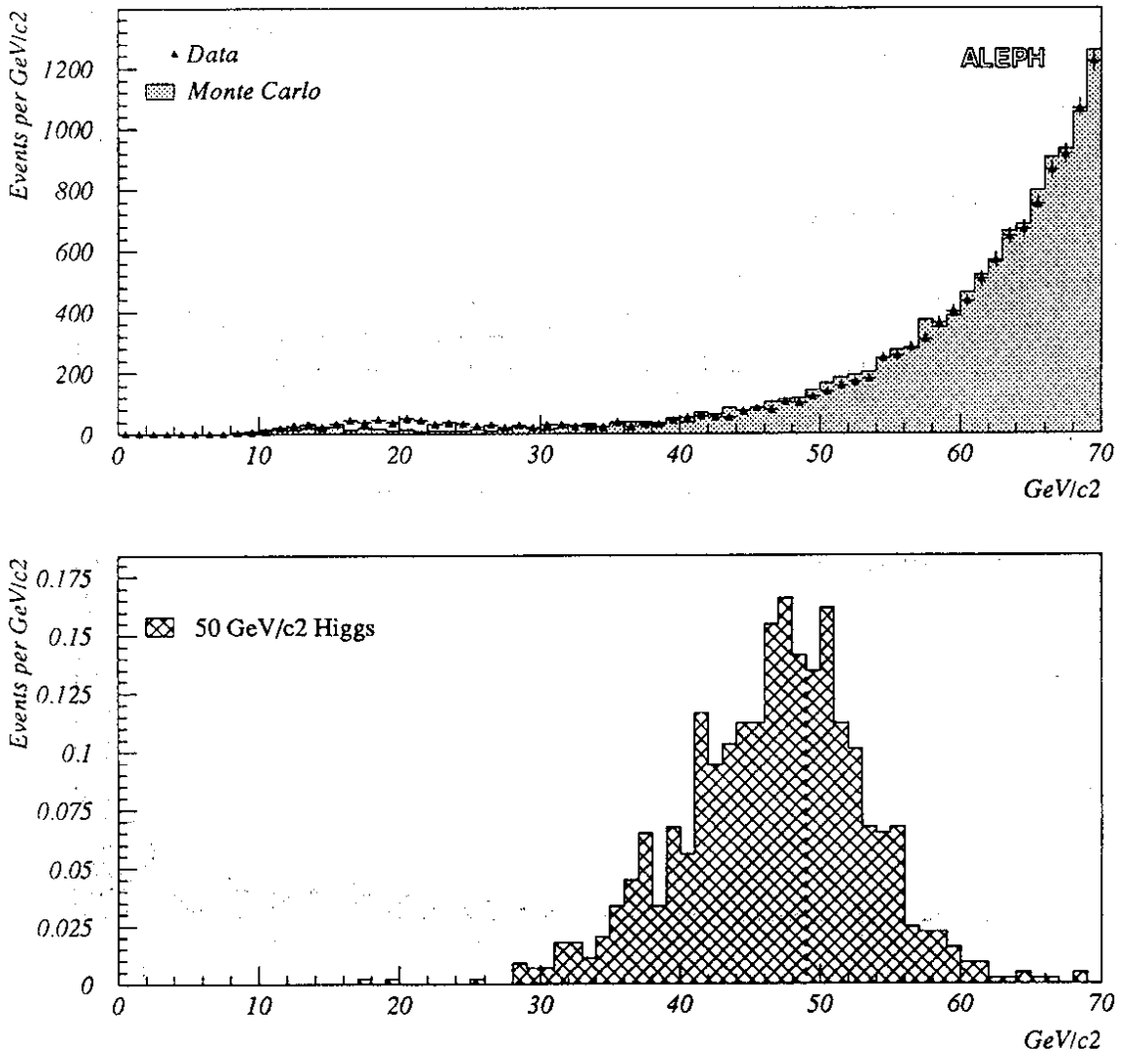

Fig.7.1 Visible mass distribution.

For a substantial fraction of these events, energy is lost because a parton has been emitted close to the beam direction and some of its fragmentation products escape the detector. This can be seen in Fig. 7.2 where the distribution of the fraction of the total visible energy that is measured beyond 30° of the beam axis is presented for the Monte Carlo prediction and for the data. After a comparison with the same distribution expected from a 50 GeV/c^2 Higgs boson, this fraction is required to exceed 60%. Furthermore, to avoid dealing with the very forward region of the detector, E_{12} has to be smaller than 3 GeV. After these requirements, leading to a 10% inefficiency for a 50 GeV/c^2 Higgs boson, 4710 events are expected and 5018 were actually observed.

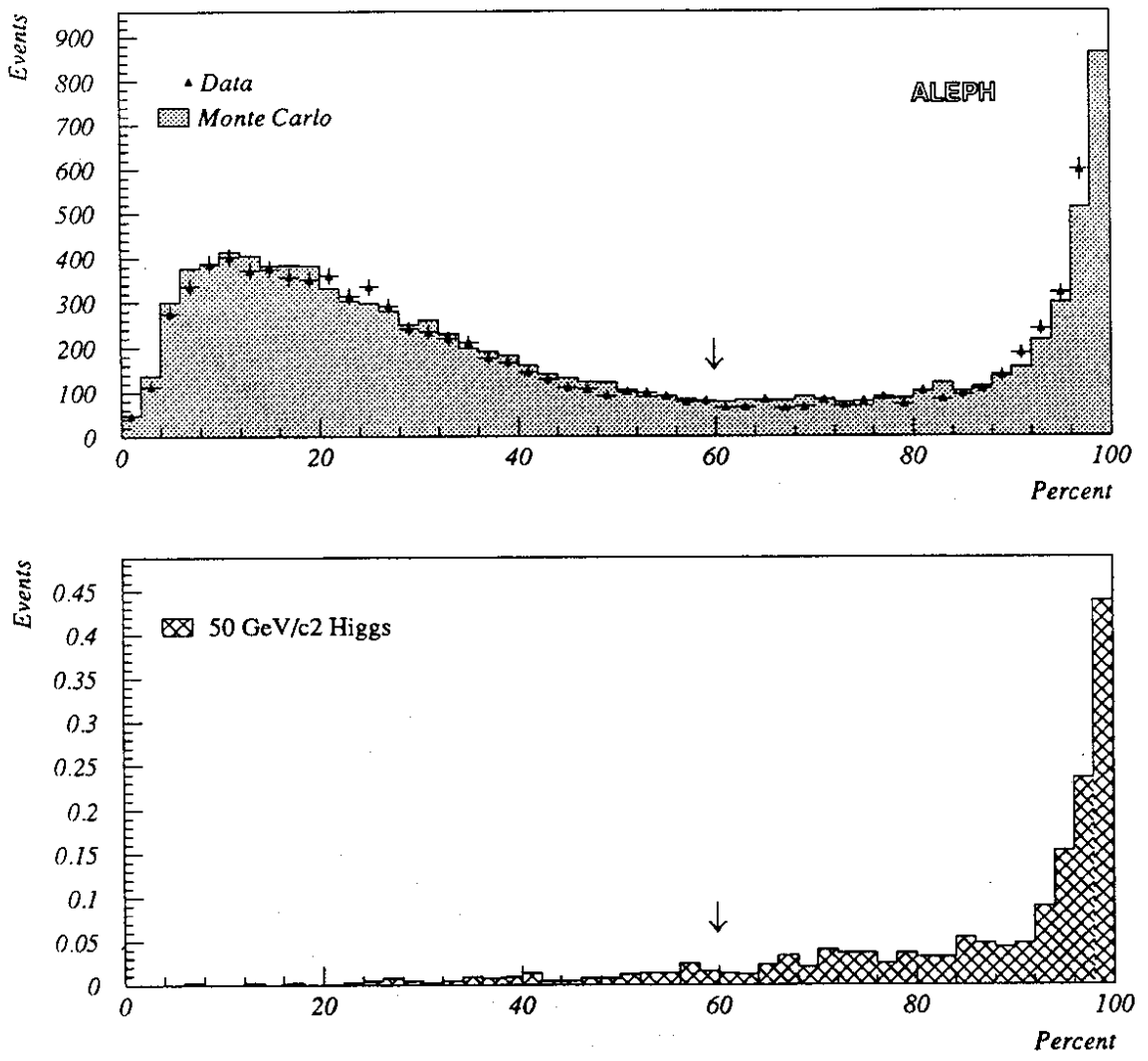

Fig.7.2 Energy fraction beyond 30 degrees.

More than 90% of the remaining background is due to $e^+e^- \rightarrow$ two jets, where at least one of the jet energies is measured to be much smaller than $\sqrt{s}/2$. This mismeasurement comes either from the energy-flow algorithm itself, in which the energy resolution is $\sim 9\%$, or from real effects like neutrino emission. As already stated, whatever the origin and the amount of energy lost, the two jets remain collinear while the two jets coming from a Higgs decay would be acollinear, as shown in Fig. 7.3. The acollinearity angle η is therefore required to be smaller than 165°. The 305 events observed satisfying this criterion are to be compared to the 354 ± 20 predicted from standard processes. The resulting inefficiency on a 50 GeV/c^2 Higgs signal is 7%.

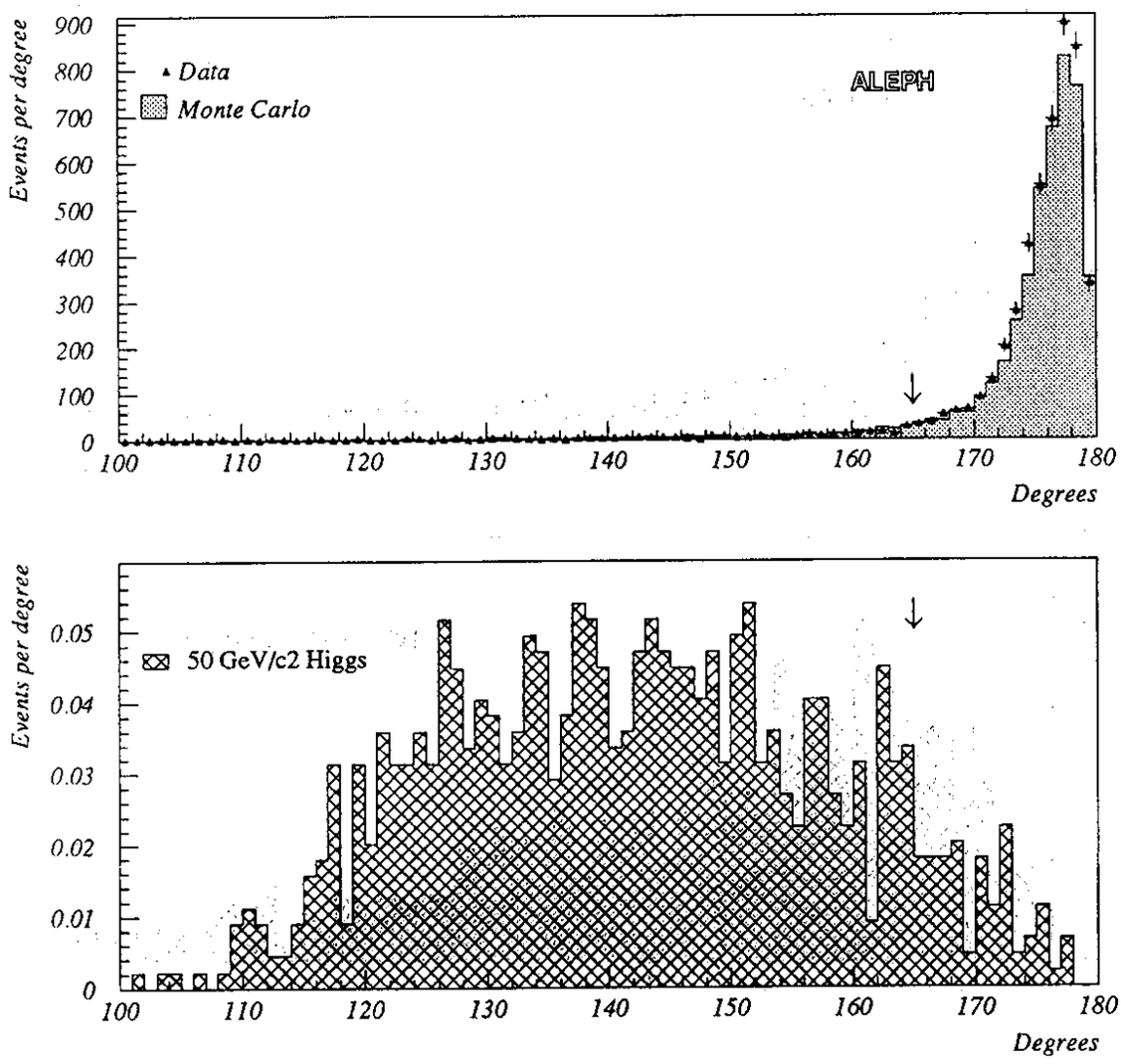

Fig.7.3 Acollinearity distribution.

However, if a hard photon radiation occurs in the initial state, the energy of this photon is lost and the two jets become acollinear. For these events, and if the jet energies were perfectly determined, the total missing momentum would point along the beam direction. Let α be the angle between the missing momentum and the beam axis (see Fig. 7.4.). To allow for some energy fluctuations in the two jets, $\tan\alpha$ is required to be larger than 0.4 ($\alpha > 21.8°$). Again half of the background disappears (155 events remained observed in the data for 180 ± 15 predicted) whereas this would affect only 4% of the signal from a 50 GeV/c^2 Higgs boson.

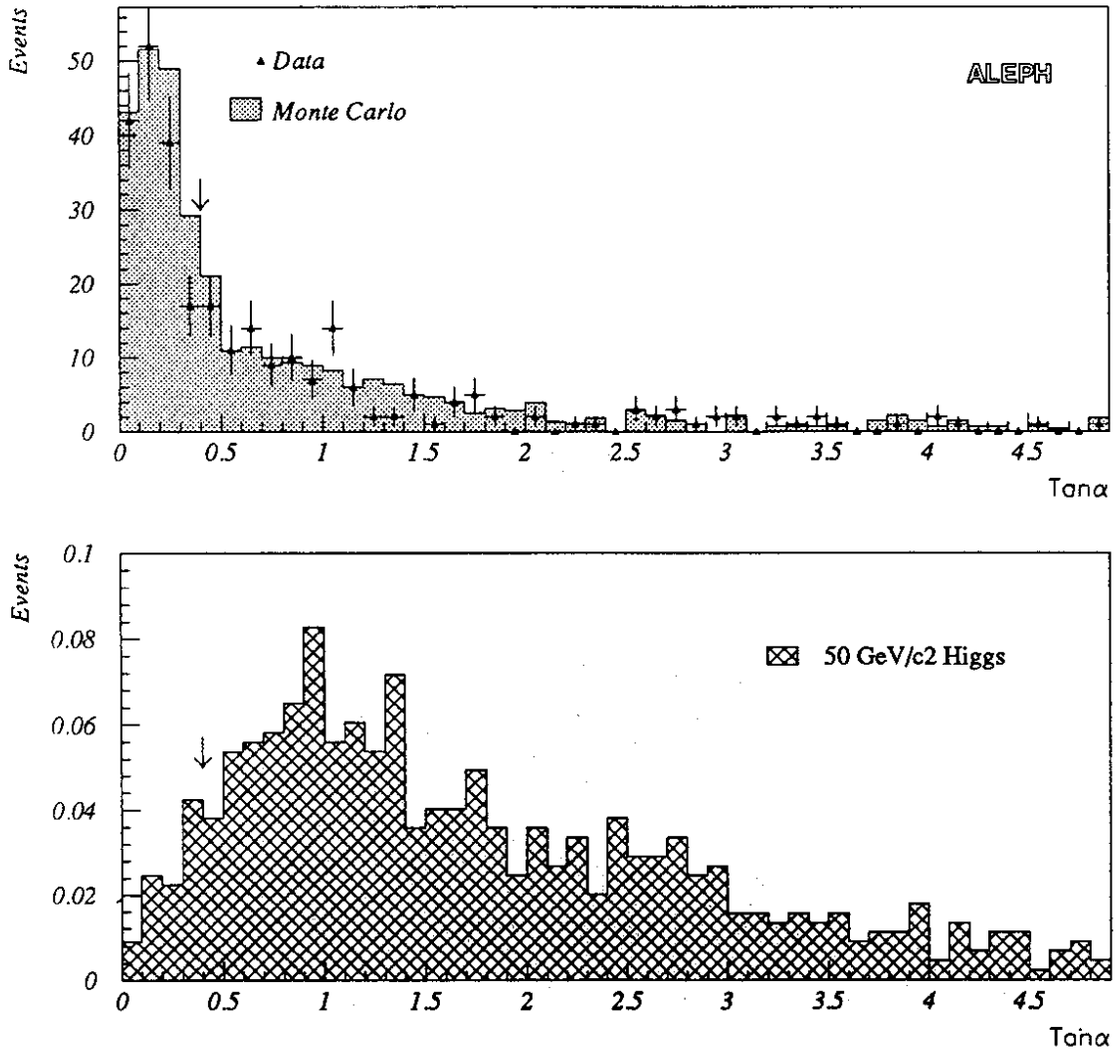

Fig.7.4 Direction of the total missing momentum.

The events surviving at this point are mostly three-jet events, where at least one of the jet energies is mismeasured, making unreliable the direction of at least one of the two hemispheres. Nevertheless, if only one jet "fluctuated", the total missing momentum should be contained in that jet, and thus not be isolated. Let E_{cone} be the total energy measured in a cone of half-angle 25.8° around the missing momentum, the distribution of which is shown in Fig. 7.5. Requiring E_{cone} to be smaller than 3 GeV introduces only a 3% additional inefficiency for the signal, but rejects again half of the background. At this stage, 95 ± 10 events are expected and 73 were actually seen.

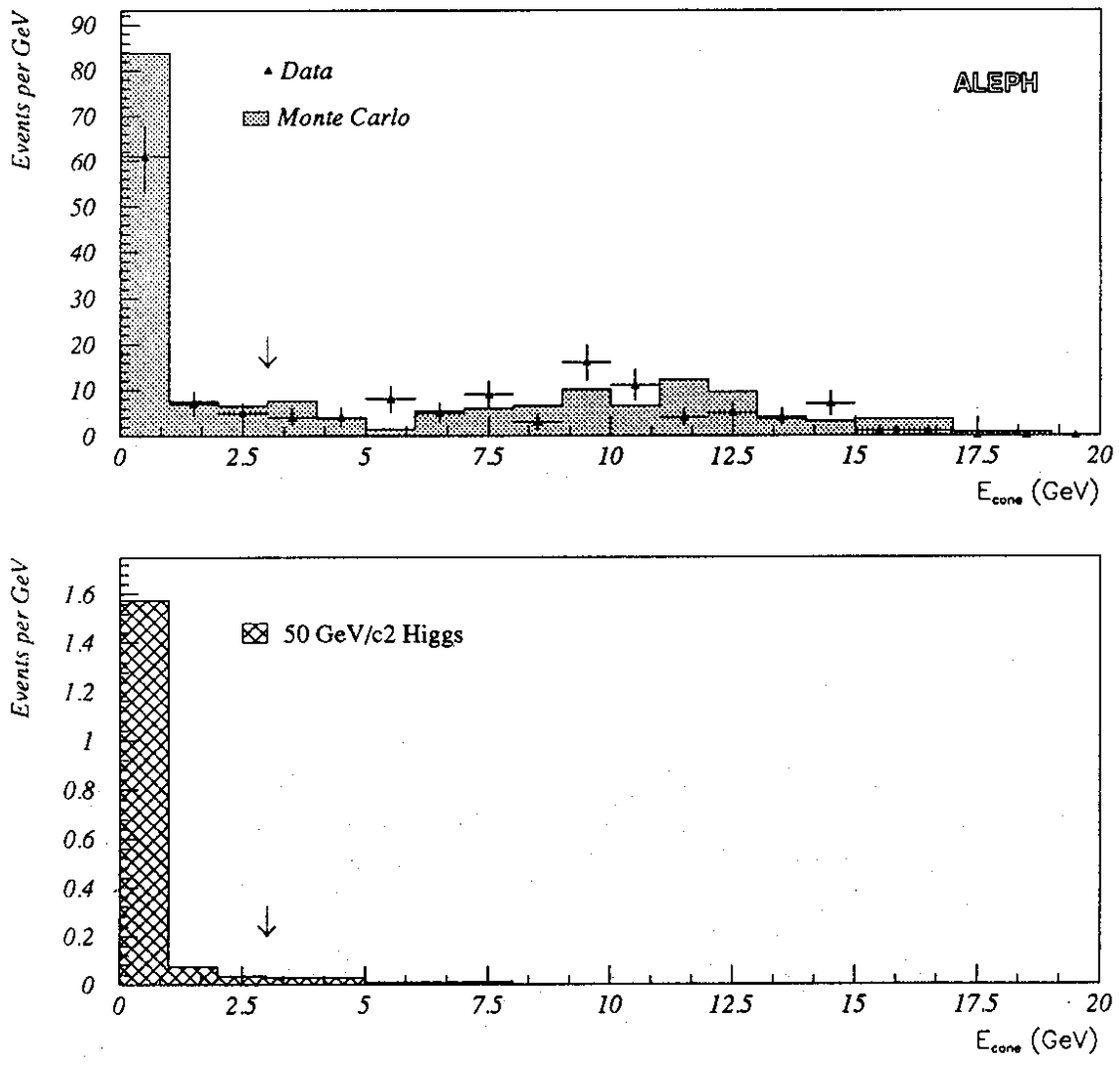

Fig.7.5 Isolation of the total missing momentum.

For three-jet events with at least two fluctuating jets, the total missing momentum direction can no longer be used, but the directions of the three jets are still well determined. Each event is thus forced into three jets, giving the directions of the three original partons. Let θ_i be the angle between the directions of jet j and jet k, with $i, j, k = 1, 2$ or 3, and with $\theta_i < 180°$. As a consequence of the total momentum conservation, the three directions have to be contained in a given plane or, in other words, have to fulfil the condition

$$\mathcal{S} = \sum_{i=1}^{3} \theta_i = 360°.$$

Two-jet events artificially forced into three-jets will tend to have a value of $\mathcal{S}$ close to 360° if collinear, but not otherwise. As, in addition, the Higgs signal events, even if three-jet like, are not expected to be planar, they always tend to be characterized by a value of $\mathcal{S}$ much smaller than 360°, as shown in Fig. 7.6.

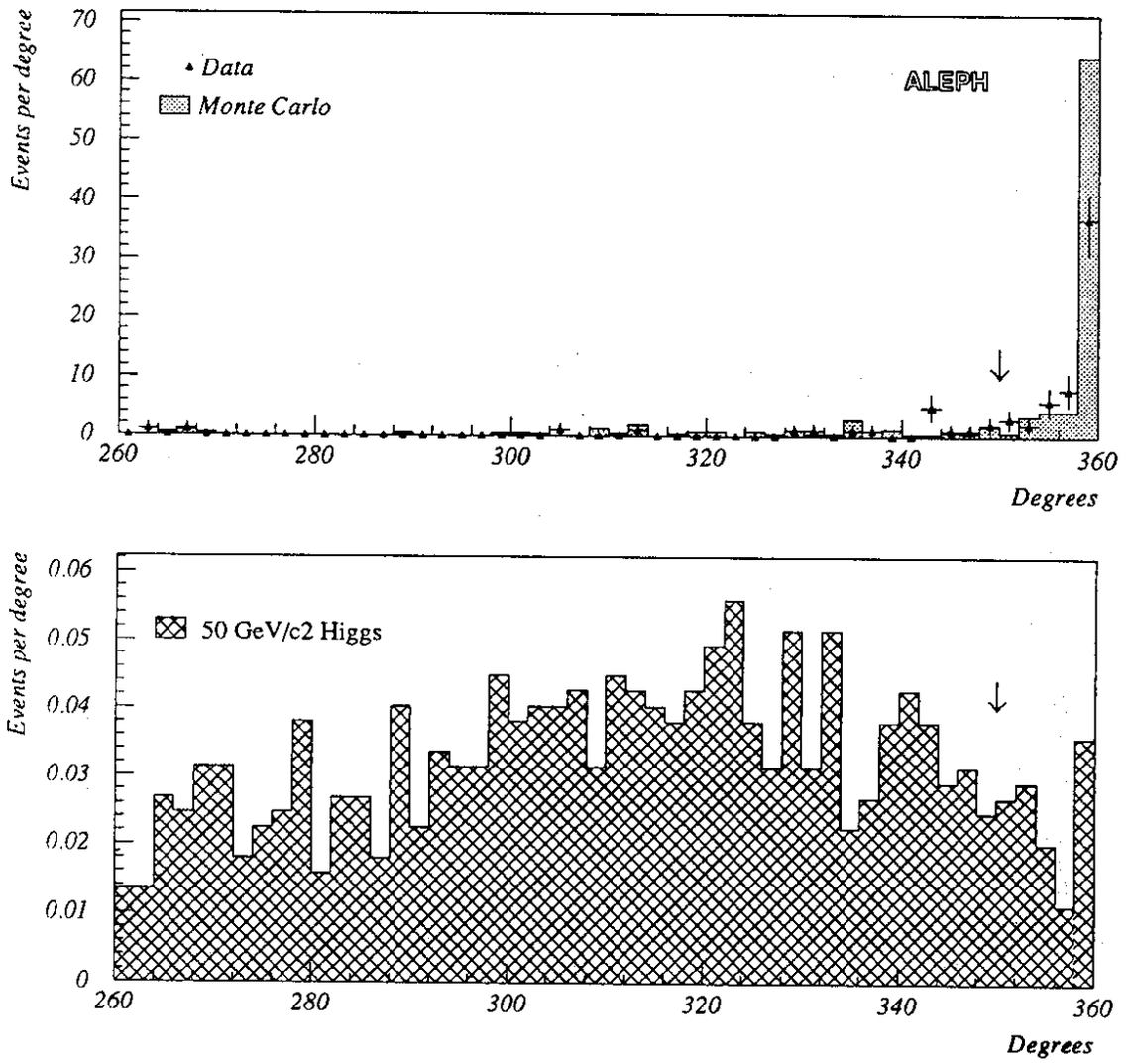

Fig.7.6 Distribution of $\mathcal{S}$.

The $q\bar{q}$ background two-jet events, which would be characterized by a small θ_i^{min}, have already been rejected by the acollinearity cut. Therefore, $\mathcal{S}$ is required to be smaller than 350°, provided the event is really three-jet like, that is when the smallest of the three angles θ_i^{min} is in excess of 40°. The two-dimensional distributions of $\mathcal{S}$ versus θ_i^{min} are presented in Fig. 7.7 for the data, for the various background sources and for a 50 GeV/c^2 Higgs. After applying the cut, 0.6 event is expected from $e^+e^- \to \tau^+\tau^-$, 6 from $e^+e^- \to q\bar{q}$ and 12 from $e^+e^- \to (e^+e^-)hadrons$, while 20 events were actually observed. The inefficiency caused by this cut amounts to 4% for a 50 GeV/c^2 Higgs boson.

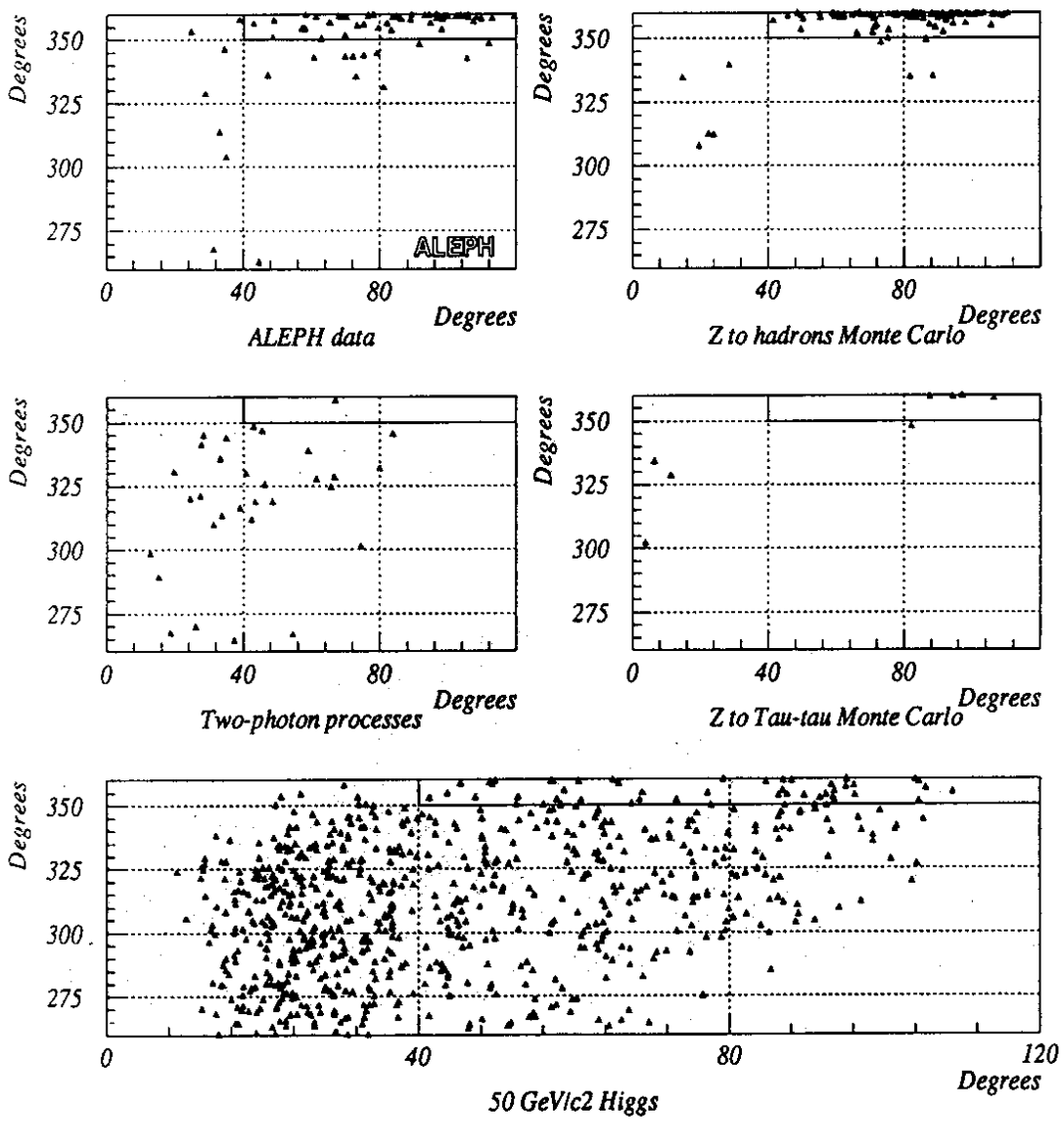

Fig. 7.7 Distribution of $\mathcal{S}$ versus θ_i^{min}.

The remaining events from $e^+e^- \to q\bar{q}$ or $\tau^+\tau^-$, characterized by a small value of θ_i^{min} (see Fig. 7.7), are two-jet events with large fluctuations and accompanied by a hard initial state radiation. Therefore, they have not been rejected by any of the previous cuts (in particular, the $\tan\alpha$ cut is inefficient because the direction of the missing momentum is no longer determined by the energetic photon only). However, making use of the direction of the two jets again, the acoplanarity angle ψ of such events remains very close to 180°, whatever the fluctuations and the photon energy, as shown in Fig. 7.8. Requiring ψ to be smaller than 175° rejects the last $q\bar{q}$ events and only 0.3 $\tau^+\tau^-$ event remains expected. At this stage, the selection efficiency is about 68% for a 50 GeV/c^2 Higgs boson.

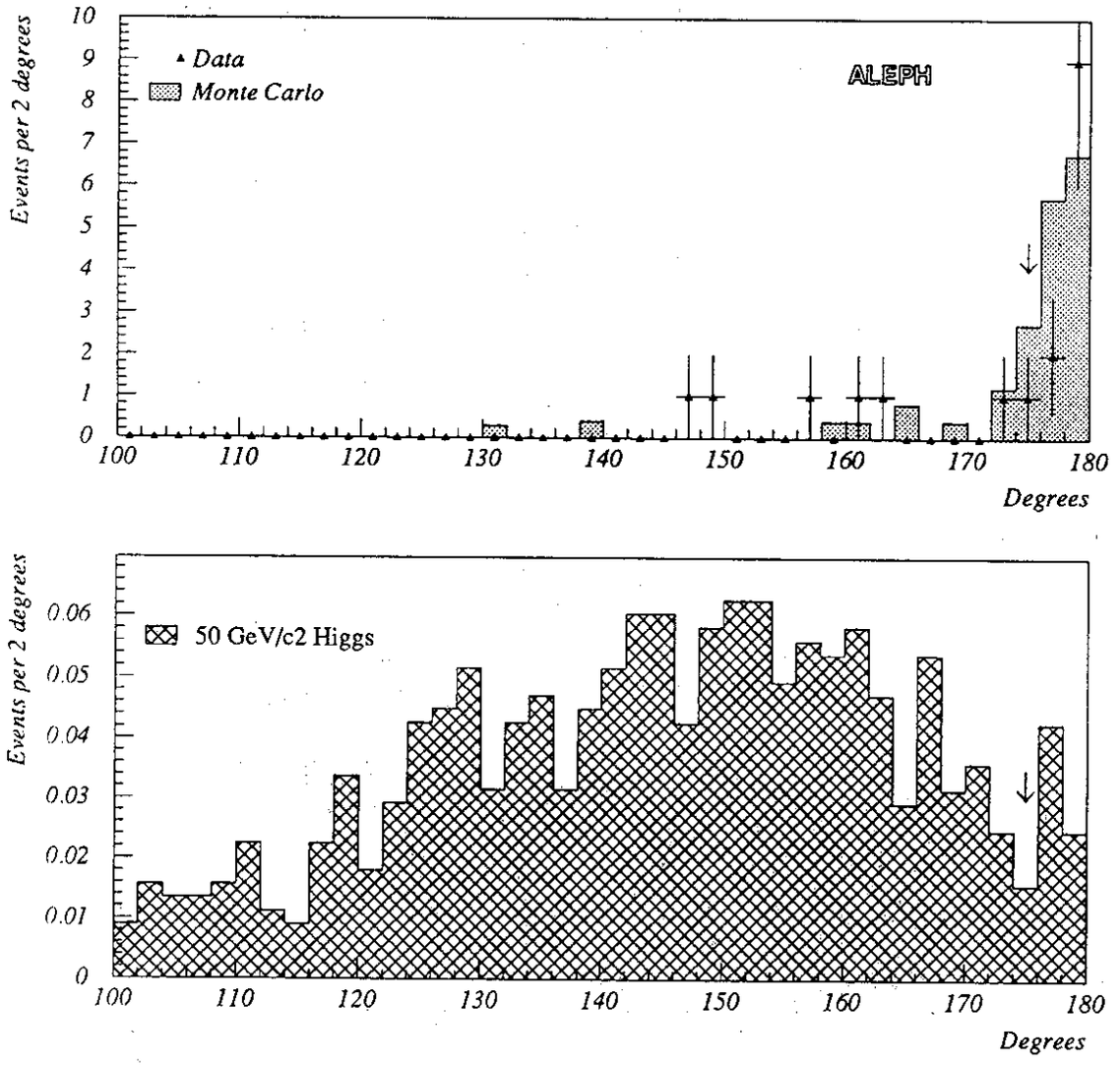

Fig.7.8 Acoplanarity distribution.

The 7 last events remaining in the data are at low visible mass and low total transverse momentum, in agreement with the 5 events expected from two-photon processes (see Fig. 7.9). It is therefore finally required, for events with a visible mass smaller than 25 GeV/c^2, that the total momentum transverse to the beam direction be larger than 5% of the centre-of-mass energy. No events remained in the data, while 0.8 is expected from two-photon processes, with no additional inefficiency for a 50 GeV/c^2 Higgs boson.

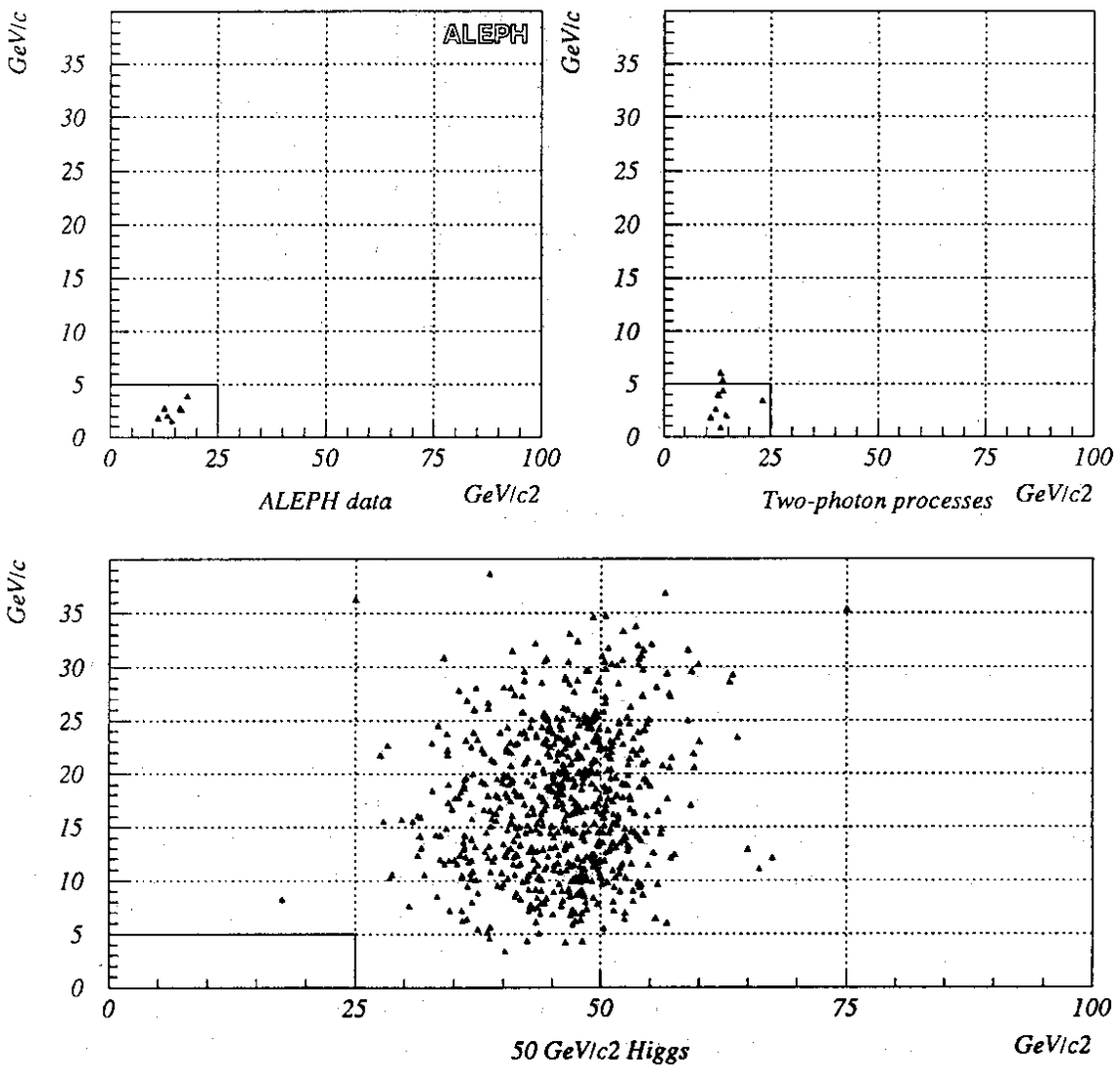

Fig.7.9 Total transverse momentum versus visible mass.

Although this analysis has been developed for events with a visible mass below 70 GeV/c^2 (see a summary in Table 2), it is worth looking at its results when applied to the full sample. No events were observed in the data over the whole mass range (rendering thus useless the 70 GeV/c^2 mass cut), while 1.4 are expected from $e^+e^- \to q\bar{q}$, but with a visible mass of $\sim$ 90 GeV/c^2.

Table 2. Effect of the cuts in the acoplanar jets analysis on the data, the background sources and a 50 GeV/c^2 Higgs signal.

Cut	Data	Backgrounds			Higgs
		$q\bar{q}$	$\tau^+\tau^-$	$\gamma\gamma$	(%)
Preselection	11,865	11,390	255	200	99.4
Low angles	5,018	4,400	225	85	90.4
Acollinearity	305	285	3	66	83.2
$\tan\alpha$	155	164	3	13	78.8
E_{cone}	73	80	2	13	75.1
$\mathcal{S}$, θ_i^{min}	19	6	1	13	71.2
Acoplanarity	7	0	0.3	4.5	67.7
p_T	0	0	0.3	0.8	67.7
No mass cut	0	1.4	0.3	0.8	67.8

In the preselection, a cut in visible mass at 70 GeV/c^2 is applied. The last line of the table gives the result of the analysis when this mass cut is removed.

When applied to the $\tau^+\tau^- q\bar{q}$ final state and for a 50 GeV/c^2 Higgs boson, the efficiencies of this search amount to 9% in the configuration $(H^0 \to \tau^+\tau^-)(Z^* \to hadrons)$ and 5% in the configuration $(H^0 \to hadrons)(Z^* \to \tau^+\tau^-)$.

8.- Search for energetic lepton pairs in hadronic events.

In this section again, the search has been optimized for a 50 GeV/c^2 Higgs boson, now in the configurations $(H^0 \to hadrons)(Z^* \to e^+e^-$ or $\mu^+\mu^-)$.

Energetic pairs, in events with at least 7 good tracks carrying more than 10% of the centre-of-mass energy, are defined as pairs of good tracks oppositely charged, with individual momenta in excess of 3 GeV/c, with a scalar sum of momenta greater than 20 GeV/c and with an invariant mass greater than 5 GeV/c^2. In the data, 62,995 events had at least one such pair for an expectation of 62,289. The efficiencies on a 50 GeV/c^2 Higgs signal are 90% and 87% in the channels $(Z^* \to \mu^+\mu^-)$ and $(Z^* \to e^+e^-)$, respectively.

To declare the pair isolated with respect to the recoiling hadronic system, first the scalar sum of the transverse momenta of the two tracks calculated with respect to the thrust axis of the rest of the event has to exceed 15 GeV/c. The distribution of this quantity is shown in Fig. 8.1 both for the data compared to the standard expectation and for the signal from a 50 GeV/c^2 Higgs. 809 events were observed after this cut (871 expected), preserving an 85% efficiency for a 50 GeV/c^2 Higgs in the channel $(Z^* \to \mu^+\mu^-)$ (80% in $Z^* \to e^+e^-$).

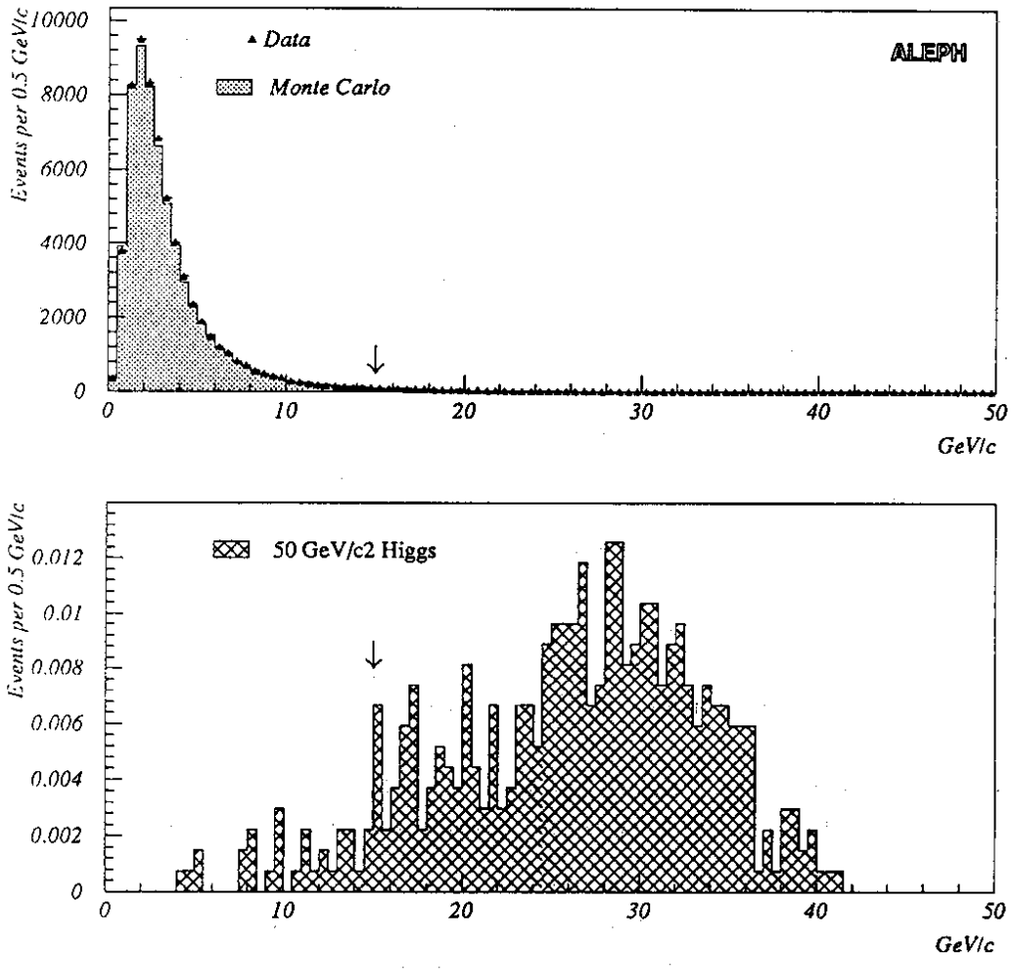

Fig.8.1 Sum of the transverse momenta of the two leptons.

In addition, at least one of the two tracks has to be topologically isolated from the other particles, that is:

- there is no other charged particle track inside a cone of 18.2° half-angle around the direction of its momentum,
- the sum of the energies of the neutral particles inside the same cone has to be smaller than 1 GeV. The clusters potentially coming from final state radiation or Bremsstrahlung photons (see Section 3) are not counted in the sum.

Only 84 events fulfilled these isolation requirements in the data, which is compatible with the 68 events expected, while the corresponding inefficiency for a 50 GeV/c^2 Higgs amounts to 5%.

Finally, in order to eliminate the remaining background events, a lepton identification is performed on both tracks, requiring one track to be "tightly" identified, and allowing the other to be only "loosely" identified:

- For the electron identification, two estimators, called R_T and R_L, constructed to have a normalized Gaussian distribution for electrons, are used. The estimator R_T compares

the momentum of the charged particle to the energy deposited in the four towers of the electromagnetic calorimeter closest to the extrapolation of the track, and the estimator R_L compares the longitudinal energy deposition of the associated cluster to a typical electromagnetic shower longitudinal profile. The tight identification is defined by $R_T > -4$ (no cut on high R_T values is applied to allow for momentum losses by Bremsstrahlung) and $|R_L| < 4$. The loose criterion requires only $R_T > -6$, except when the charged particle track extrapolates to an ECAL crack, where R_T cannot be calculated reliably; in that case, the associated HCAL cluster, if any, must have fewer than 6 planes of streamer tubes fired.

- For the muon identification, the track is extrapolated through the HCAL up to the muon chambers, and the number of planes fired inside a road 5 cm-wide around the extrapolation of the track is compared to the number of instrumented planes in the corresponding HCAL region. The tight identification criterion requires, in regions where at least 15 planes are instrumented, at least a third of them to be fired, and at least 1 hit to be registered in the last three HCAL planes or in the muon chambers. The loose identification criterion requires:

  a) in regions where at least 10 planes are instrumented, at least one hit in the last 10 HCAL planes or in the muon chambers and less than 15 GeV in the corresponding HCAL cluster;

  b) in regions where fewer than 10 planes are instrumented or for the tracks with a momentum smaller than 5 GeV/c, no associated ECAL cluster or $R_T < -5$.

Requiring the two tracks to be two electrons or two muons, of which at least one is tightly identified, has an efficiency of 92% on the signal, in both ($Z^* \rightarrow \mu^+\mu^-$) and ($Z^* \rightarrow e^+e^-$). No events remained in the data while 0.7 $e^+e^- \rightarrow q\bar{q}$ event is expected. The overall efficiency of the selection for a 50 GeV/c^2 Higgs boson is 74% in the channel ($Z^* \rightarrow \mu^+\mu^-$) and 69% in the channel ($Z^* \rightarrow e^+e^-$).

A control analysis has been performed by looking for an $H^0e\mu$ signal in the data, requiring two leptons of which at least one is tightly identified, thus providing the possibility of testing the lepton identification criteria on an independent sample. The deep inelastic scattering (with one tagged electron) was pointed out by this check to be the main background to the $H^0e\mu$ final state (3.6 events expected, 3 events seen), and even to the H^0ee final state although the loose electron identification is much more selective against soft pions than the loose muon one (1.2 event expected, 0 event seen). In order to eliminate this ultimate background, it has therefore been required, in the final states with one electron tightly identified, that $Q_e.p_L$ be smaller than $15\%\sqrt{s}$, where p_L is the missing longitudinal momentum of the event and Q_e the sign of the charge of the most energetic electron. No $H^0e\mu$ events remained in the data, while 0.4 deep inelastic scattering event (with two tagged electrons) is expected. This last cut introduces less than half a percent of additional inefficiency for a 50 GeV/c^2 Higgs in the channel ($Z^* \rightarrow e^+e^-$).

Applying these analyses to the $\tau^+\tau^-q\bar{q}$ final state for a 50 GeV/c^2 Higgs boson, the efficiencies are 7% in the configuration ($H^0 \rightarrow \tau^+\tau^-$)($Z^* \rightarrow$ *hadrons*) and 4% in the configuration ($H^0 \rightarrow$ *hadrons*)($Z^* \rightarrow \tau^+\tau^-$). These are to be added to the 9% and 5% obtained in Section 7.

9.- Search for isolated charged particle pairs in hadronic events.

In this section, the search has been optimized for a 50 GeV/c^2 Higgs boson, in the configurations $(H^0 \rightarrow hadrons)(Z^* \rightarrow \tau^+\tau^-)$ and $(H^0 \rightarrow \tau^+\tau^-)(Z^* \rightarrow hadrons)$, when the two *taus* do not decay necessarily into leptons. In that case, the lepton identification can no longer be used and the isolation requirements have to be tightened to reject the background.

Only events with at least 7 good tracks carrying more than 10% of the centre-of-mass energy are considered in the analysis. At least two oppositely charged particles, with momenta $p_1 > 2.5$ GeV/c and $p_2 > 5$ GeV/c and with polar angles between 45° and 135°, have to be isolated from the other particles. To be isolated, a particle has to fulfil the following conditions: there is no other charged particle tracks inside a cone of half-angle 25.8° around the direction of its momentum; the invariant mass of the particles contained in the cone has to be compatible with the *tau* mass, i.e. smaller than 1.5 GeV/c^2.

Only 57 events survived these cuts in the data, with 26 expected from $e^+e^- \rightarrow q\bar{q}$. However, there is no particular reason to observe any missing energy in these background events, while some missing energy is expected in the signal events due to the neutrinos coming from the *tau* decays (see Fig. 9.1).

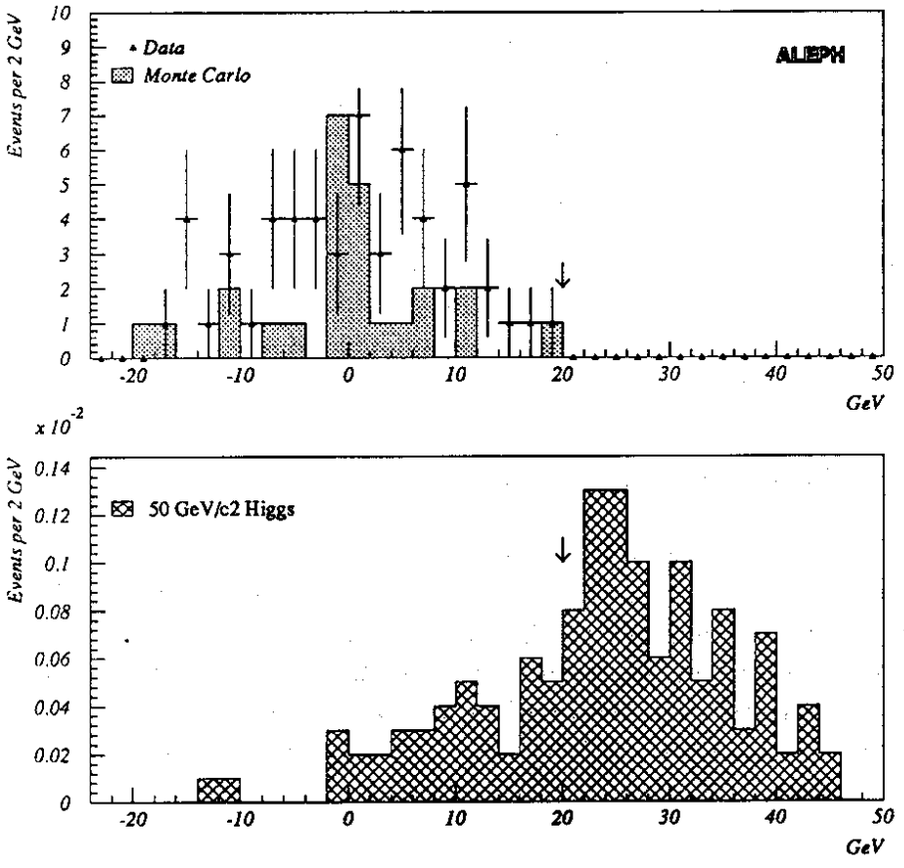

Fig.9.1 Missing energy distribution.

Therefore, a missing energy of at least 20 GeV is required, eliminating the remaining simulated background and leading to 0 event in the data.

For a 50 GeV/c^2 Higgs boson, the efficiencies of this selection are 10% in the $(H^0 \rightarrow \tau^+\tau^-)(Z^* \rightarrow hadrons)$ channel and 4% in the $(H^0 \rightarrow hadrons)(Z^* \rightarrow \tau^+\tau^-)$ channel, bringing additional efficiencies of 6.5% and 3% to the 16% and 9% obtained with the analyses presented in Sections 7 and 8.

10.- Search for an isolated charged particle in hadronic events.

In this section, the topology which is searched for is a charged particle accompanied by missing energy and momentum, both isolated from a hadronic system. Appropriate selection criteria have been developed and optimized to search for charged Higgs bosons in the channel $e^+e^- \rightarrow H^+H^- \rightarrow (c\bar{s})(\tau^-\bar{\nu}_\tau)$. This analysis is found to increase the selection efficiency in the configurations $(H^0 \rightarrow \tau^+\tau^-)(Z^* \rightarrow hadrons)$ and $(H^0 \rightarrow hadrons)(Z^* \rightarrow \tau^+\tau^-)$ when the energy of one of the *taus* is mostly carried away by decay neutrinos.

Only events with at least 6 charged particles carrying more than 10% of the centre-of-mass energy are considered. At least one charged particle with a momentum in excess of 2.5 GeV/c and with a polar angle between 45° and 135° has to be isolated from the other particles (with the same definition as in Section 9). This preselection led to 4929 events.

To select further events with isolated missing energy and momentum, the total transverse missing momentum of the event with respect to the beam axis is required to exceed 7 GeV/c and the total missing energy has to be larger than 10 GeV. Furthermore, the total energy measured in a cone of half angle 25.8° around the total missing momentum of the event has to be smaller than 3 GeV. The effect of this cut is shown on Fig. 10.1. At this stage, 21 events remained in the data while 29 are expected.

Since, in the Higgs mass domain of interest here (40 GeV/c^2 $\lesssim m_{H^0} \lesssim$ 50 GeV/c^2), the standard Higgs boson and the Z^* also carry about half of the centre-of-mass energy each, the energy of the hadronic system (recoiling against the *tau*-cone) is expected to be $\sim$ 45 GeV; it is thus required to be smaller than 55 GeV, but no lower bound has been applied in order to allow for energy losses due to additional neutrinos for instance.

No events remained in the data after this cut, but a few background events survive in the Monte-Carlo sample. Those are eliminated by observing that they are 3-jet events with a mismeasured missing momentum but in which the planar topology is preserved (while such a feature is not expected in the H^0Z^* signal). To determine the directions of the "non-*tau*" jets, the event, from which the *tau*-cone has been removed, is forced into two jets. Let S be the sum of the angles between the *tau* and the first jet, between the *tau* and the second jet, and between the two jets; S is expected to be close to 360° for planar events but not otherwise. A cut on S at 359.5° eliminates all of the 3.5 expected events.

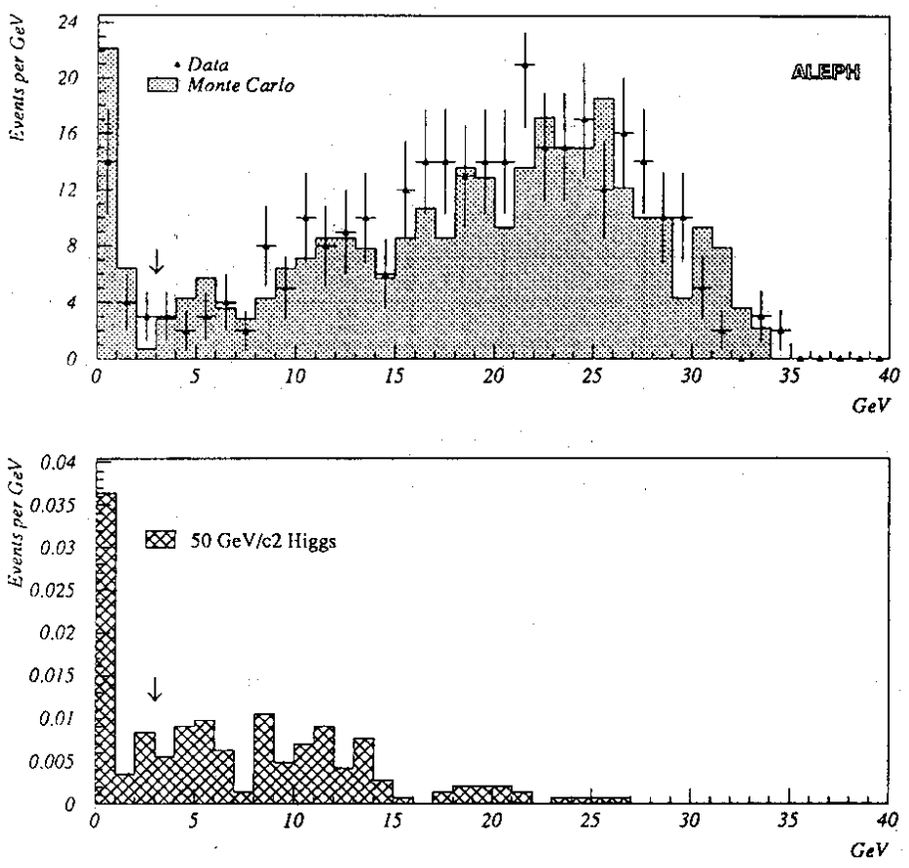

Fig.10.1 Isolation of the missing momentum.

For a 50 GeV/c^2 neutral Higgs boson, the efficiencies of the analysis are 7% in the $(H^0 \rightarrow \tau^+\tau^-)(Z^* \rightarrow hadrons)$ channel and 5% in the $(H^0 \rightarrow hadrons)(Z^* \rightarrow \tau^+\tau^-)$ channel, bringing additional efficiencies of 3.5% and 3% to the 22.5% and 12% obtained with the analyses presented in Sections 7, 8 and 9.

11.- Search efficiencies and numbers of events expected from $e^+e^- \rightarrow H^0Z^*$.

11.a.- Very low mass domain : $0 \leq m_{H^0} < 2m_\mu$.

In this mass range, only two of the analyses presented above contribute. The search for energetic acoplanar pairs presented in Section 3 applies for very light Higgs bosons which escape undetected, accompanied by a pair of electrons or muons from the Z^* decay. For higher masses, the Higgs lifetime becomes shorter so that some of the decays are expected to occur close enough to the interaction vertex for the search for acoplanar pairs described in Section 4 to be efficient in the configuration $(H^0 \rightarrow e^+e^-)(Z^* \rightarrow \nu\bar{\nu})$. Table 3 shows the efficiencies of these two analyses as a function of the Higgs mass. The numbers of events expected are presented in that same table and in Fig. 11.1. The total number of events expected exceeds 38 in the Higgs mass range considered, allowing this domain to be excluded at a confidence level much higher than 95%.

Table 3. Efficiencies and expected numbers of events for the two complementary acoplanar pair searches in the very low Higgs mass domain.

	$H^0\nu\bar{\nu}$		$H^0e^+e^-$		$H^0\mu^+\mu^-$	
m_{H^0} (MeV/c^2)	Eff. (%)	N_{exp}	Eff. (%)	N_{exp}	Eff. (%)	N_{exp}
0	–	–	20.	17	30.	26
25	1.	5	16.	14	24.	21
50	3.	16	10.	9	15.	13
75	6.	31	5.	4.3	8.	6.5
100	9.	47	2.	1.7	3.	2.6
125	14.	73	1.	0.9	1.5	1.3
150	20.	104	–	–	–	–
200	28.	145	–	–	–	–
212	49.	253	–	–	–	–

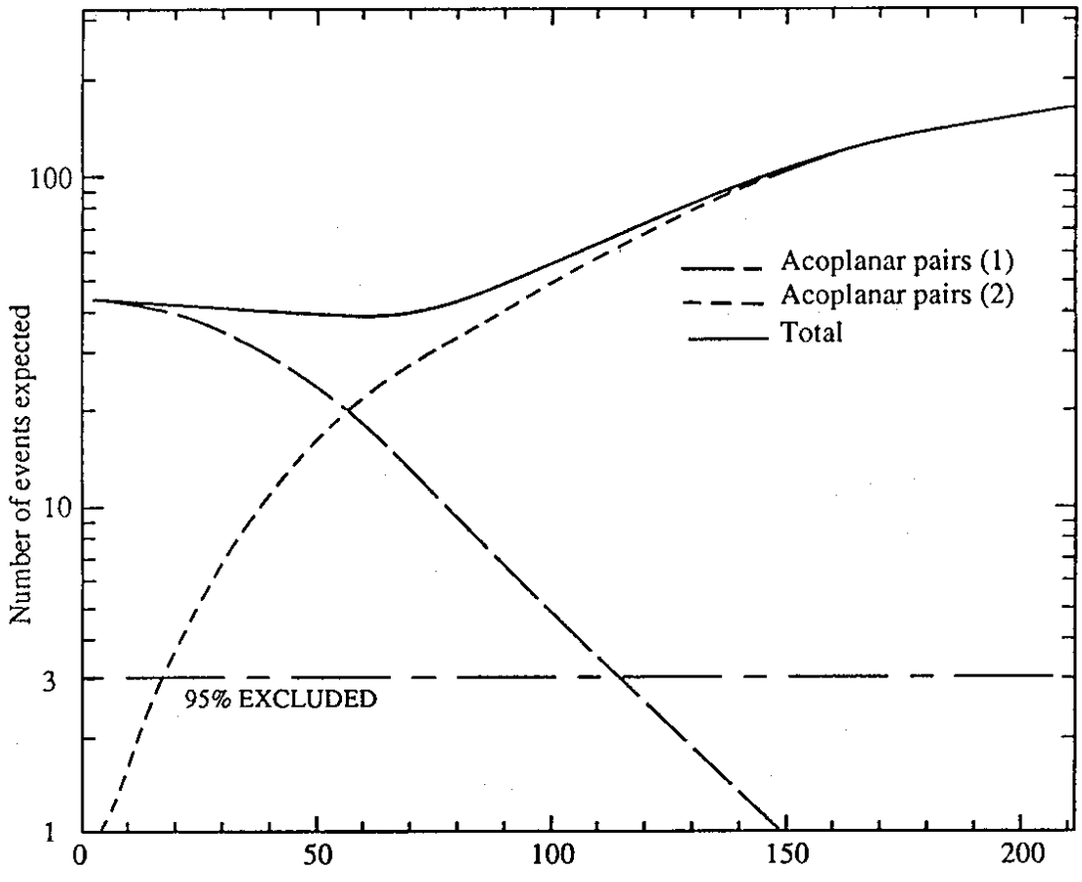

Fig.11.1 Number of events expected below the muon threshold.

11.b.- Intermediate mass domain : $2m_\mu < m_{H^0} < 15\ GeV/c^2$.

Between the muon threshold and ~ 15 GeV/c^2, the most relevant analyses are the acoplanar pair and the monojet searches applied to the $H^0\nu\bar{\nu}$ channel. The acoplanar pair selection is naturally efficient when the Higgs decays mostly into two or four charged particles, that is for masses below the $D\overline{D}$ threshold. The additional efficiency brought by the monojet analysis increases progressively with the Higgs mass, as shown in Table 4. Fig. 11.2 shows the corresponding numbers of events expected to be observed if the Higgs mass were between $2m_\mu$ and 15 GeV/c^2. In the whole mass range, a total of at least 32 events are expected while none was seen, allowing this domain to be excluded with more than 95% confidence.

Table 4. Efficiencies and expected numbers of events for the acoplanar pair and monojet searches for the Higgs mass between $2m_\mu$ and 15 GeV/c^2. ($H^0\nu\bar{\nu}$ channel only)

	Acoplanar pairs		Monojets	
m_{H^0} (GeV/c^2)	Eff. (%)	N_{exp}	Eff. (%)	N_{exp}
0.212	49.	253	–	–
0.300	36.	184	–	–
0.500	38.	189	–	–
0.800	35.	165	–	–
1.0	33.	149	–	–
1.2	32.	139	–	–
1.4	30.	125	0.5	2.1
1.6	31.	124	0.5	2.0
1.8	35.	134	1.	3.8
2.0	33.	121	2.	7.3
2.5	38.	125	4.	13
3.0	32.	96	9.	27
4.0	21.	52	26.	65
5.0	19.	41	28.	60
8.0	13.	19	40.	58
11.0	11.	11	42.	45
15.0	2.	1.3	43.	31

The efficiencies and the numbers of events given for the monojet search are to be understood as additional to the corresponding quantities in the acoplanar pair search.

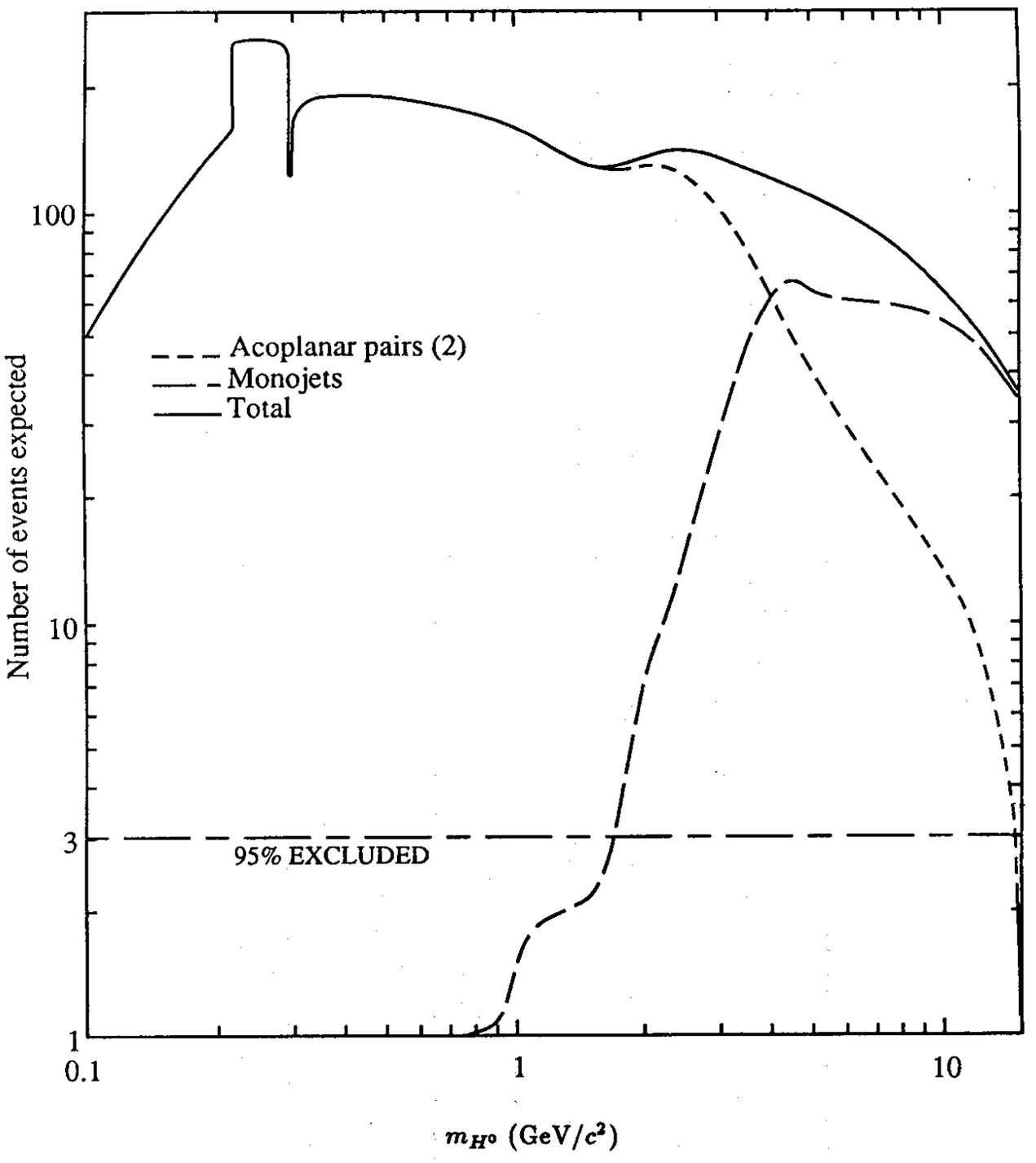

Fig.11.2 Number of events expected between the muon threshold and 15 GeV/c^2.

11.c.- High mass domain : $m_{H^0} > 11$ GeV/c^2.

In order to be sensitive to the highest possible Higgs mass, all the topologies presented in this paper have been included to derive the final result. The most important final state (18.8% of the cases) is the $(H^0 \rightarrow hadrons)(Z^* \rightarrow \nu\bar{\nu})$ channel, leading to a monojet or an acoplanar pair of jets (see Sections 6 and 7). The other final states like *hadrons* l^+l^- (3.1% for each lepton $l = e$ or μ, see Section 8), *hadrons* $\tau^+\tau^-$ and $\tau^+\tau^-$ *hadrons* (7.3%, see Sections 7, 8, 9 and 10), $\tau^+\tau^-$ $\nu\bar{\nu}$ (1.2%, see Section 4) and $\tau^+\tau^-$ l^+l^- (0.6%, see Section 5), also contribute significantly. The efficiencies of the corresponding analyses for each channel are listed in Table 5 together with the numbers of events expected to be found. The latter are summarized in Fig 11.3. The total number of events expected for a 48 GeV/c^2 Higgs boson is 3.05. With no events observed, such a Higgs boson is excluded with 95% confidence.

Table 5. Efficiencies and expected numbers of events for all the final states considered when $m_{H^0} > 11$ GeV/c^2.

5.1 - $H^0 \rightarrow hadrons$.

	$Z^* \rightarrow \nu\bar{\nu}$		$Z^* \rightarrow e^+e^-$		$Z^* \rightarrow \mu^+\mu^-$		$Z^* \rightarrow \tau^+\tau^-$	
m_{H^0} (GeV/c^2)	(%)	N_{exp}	(%)	N_{exp}	(%)	N_{exp}	(%)	N_{exp}
11	65.	54.5	60.	7.9	71.	9.4	21.	2.82
20	69.	29.5	70.	4.95	78.	5.51	22.	1.49
30	75.	13.2	75.	2.15	82.	2.35	23.	0.66
40	77.	5.11	73.	0.80	80.	0.88	20.	0.22
48	71.	1.99	71.	0.33	76.	0.36	17.	0.08
50	68.	1.49	69.	0.25	74.	0.27	15.	0.05
60	54.	0.31	63.	0.06	67.	0.06	7.	0.01

5.2 - $H^0 \rightarrow \tau^+\tau^-$.

	$Z^* \rightarrow hadrons$		$Z^* \rightarrow \nu\bar{\nu}$		$Z^* \rightarrow l^+l^-$	
m_{H^0} (GeV/c^2)	(%)	N_{exp}	(%)	N_{exp}	(%)	N_{exp}
11	7.	6.36	41.	11.0	54.	7.16
20	11.	1.03	41.	1.14	54.	0.73
30	17.	0.65	41.	0.46	54.	0.30
40	24.	0.35	41.	0.18	54.	0.11
48	26.	0.16	41.	0.08	54.	0.05
50	26.	0.12	41.	0.06	54.	0.04
60	25.	0.03	32.	0.01	54.	0.01

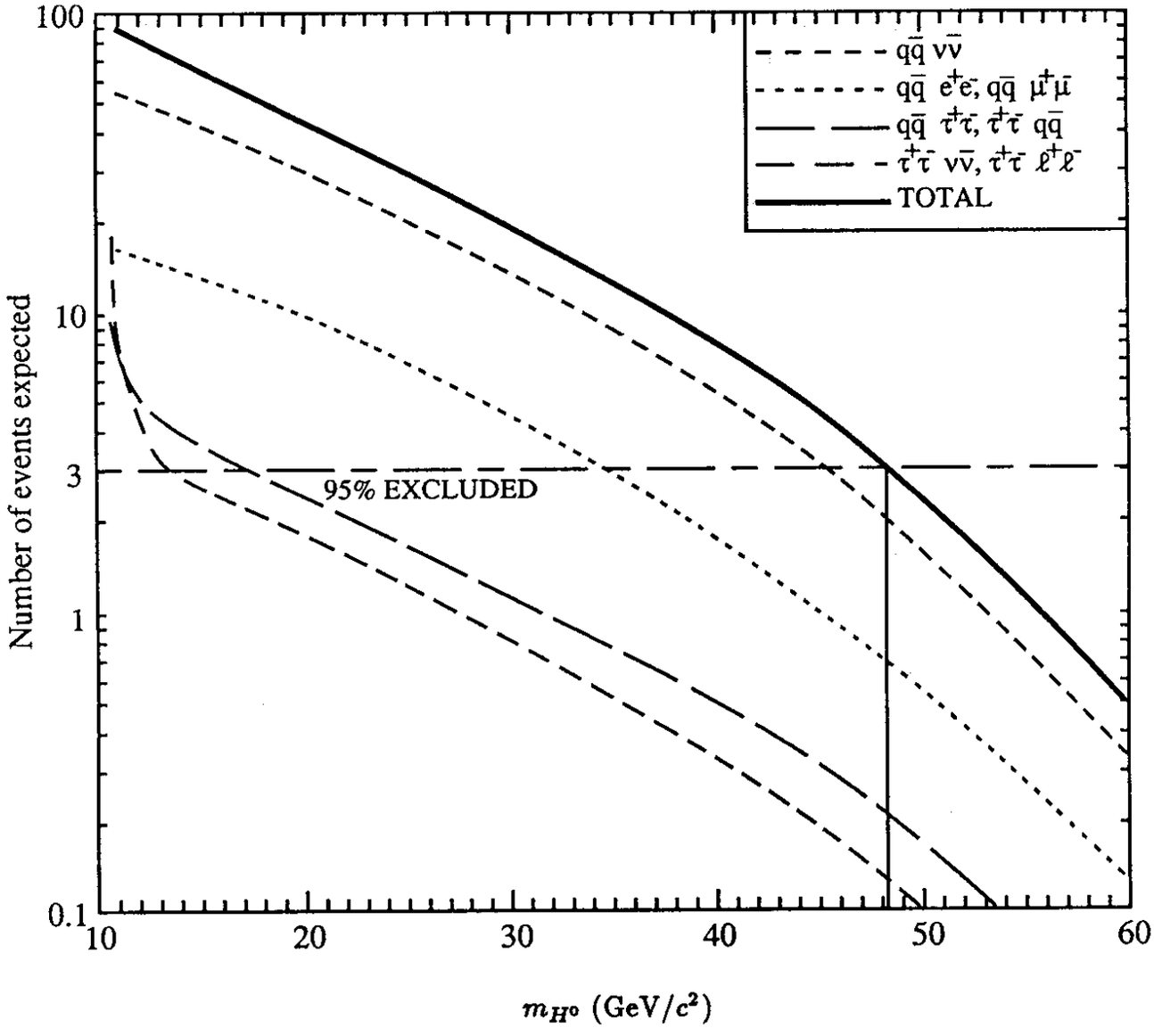

Fig.11.3 Number of events expected between 11 GeV/c^2 and 60 GeV/c^2.

11.d.- Systematics.

No detailed systematic studies have been performed in the very low mass and in the intermediate mass domains since the total number of events expected to be seen is so large. In the high mass domain, about 85% of the Higgs events expected to be found come from the configurations $(H^0 \rightarrow hadrons)(Z^* \rightarrow \nu\bar{\nu},\ e^+e^-$ or $\mu^+\mu^-)$. The systematic errors have therefore been studied carefully for these final states only and assumed to be of the same order for the other channels (the relative contributions from these channels are very small, and the dominant systematic errors are common to all the channels).

The uncertainty on the number of multihadronic events in the data sample induces a systematic error of 0.6% (see Section 2.h). Another source of systematic error is the dependence on the *top* mass of the $e^+e^- \rightarrow H^0Z^*$ cross section: varying m_{top} from 90 to 200 GeV/c^2 gives rise to a $\sim$ 1% variation in the ratio of the $q\bar{q}$ to H^0Z^* cross sections. The limited Higgs Monte Carlo statistics introduces a contribution of 0.7% to the error.

The most important uncertainty might originate from the hadronization of the $q\bar{q}$ pair coming from a scalar particle (the Higgs boson). In order to determine this uncertainty, the Higgs decay simulation has been performed both using the $H^0 \rightarrow q\bar{q}g$ matrix element and applying the Lund parton shower evolution to the quark pair, pretending thus that the two quarks are produced from a vector boson. This results in a variation smaller than 0.5% in the selection efficiencies. A 0.5% additional error has been estimated by varying the QCD and fragmentation parameters (mainly $\Lambda_{QCD}, \sigma_q, \epsilon_b$).

The electron and muon identification efficiencies ($H^0l^+l^-$ channel only) have been compared in the data and in the simulation with samples of Bhabha and dimuon events. The difference between the data and the Monte Carlo has been shown to be smaller than 1%.

Adding the various uncertainties in quadrature, a total systematic error of 2% is obtained. Conservatively reducing by this amount the total number of events expected to be observed, the Higgs mass lower limit obtained is 48 GeV/c^2.

12.- Conclusion.

Using a data sample corresponding to approximately 185,000 hadronic Z decays, the process $e^+e^- \rightarrow H^0Z^*$ has been studied in most of the possible final states in order to search for the Standard Higgs boson H^0. No events have been found in any of these analyses, thus allowing an extension to higher masses of the domain previously excluded by ALEPH[4] and other LEP experiments.[5] Combining all the analyses presented here, the whole Higgs mass range between 0 and 48 GeV/c^2 is excluded at the 95% confidence level. When the present analyses are applied to higher statistics, they will be sensitive to a 60 GeV/c^2 Higgs boson with the million events which is foreseen to be recorded in 1991.

Acknowledgements.

We wish to congratulate and thank our colleagues in the LEP Division for the remarkable performance of the LEP accelerator. We also thank the engineers and technicians in all our institutions for their support in constructing and operating ALEPH. Those of us from non-member countries thank CERN for its hospitality.

References.

1. D. Decamp et al., (ALEPH Coll.), *Phys. Lett.* **236B** (1990), 233.
2. D. Decamp et al., (ALEPH Coll.), *Phys. Lett.* **241B** (1990), 141.
3. D. Decamp et al., (ALEPH Coll.), *Phys. Lett.* **245B** (1990), 289.
4. D. Decamp et al., (ALEPH Coll.), *Phys. Lett.* **246B** (1990), 306.
5. P. Abreu et al., (DELPHI Coll.), *Nucl. Phys.* **B342** (1990), 1,
   P. Abreu et al., (DELPHI Coll.), CERN -PPE/90-163, November 1990,
   P. Abreu et al., (DELPHI Coll.), CERN -PPE/90-193, December 1990,
   B. Adeva et al., (L3 Coll.), *Phys. Lett.* **248B** (1990), 203,
   B. Adeva et al., (L3 Coll.), L3 preprint #19, September 1990,
   B. Adeva et al., (L3 Coll.), L3 preprint #24, December 1990,
   M. Akrawy et al., (OPAL Coll.), *Phys. Lett.* **236B** (1990), 224,
   M. Akrawy et al., (OPAL Coll.), CERN-PPE/90-100, June 1990,
   M. Akrawy et al., (OPAL Coll.), *Phys. Lett.* **251B** (1990), 211,
   M. Akrawy et al., (OPAL Coll.), CERN -PPE/90-150, October 1990.
6. D. Decamp et al., (ALEPH Coll.), *Nucl. Inst. and Methods* **A294** (1990), 121.
7. T. Sjöstrand, *Comput. Phys. Commun.* **28** (1983), 229.
8. D. Decamp et al., (ALEPH Coll.), *Phys. Lett.* **231B** (1989), 519.

Imprimé au CERN. Prix : 0.75 Fr.